

**GUGGENHEIM AERONAUTICAL LABORATORY
CALIFORNIA INSTITUTE OF TECHNOLOGY**

HYPERSONIC RESEARCH PROJECT

Memorandum No. 63

September 15, 1961

**HOT-WIRE MEASUREMENTS IN
LOW REYNOLDS NUMBER HYPERSONIC FLOWS**

by

C. Forbes Dewey, Jr.



**ARMY ORDNANCE CONTRACTS
DA-04-495-Ord-1960 and DA-04-495-ORD-3231**

GUGGENHEIM AERONAUTICAL LABORATORY
CALIFORNIA INSTITUTE OF TECHNOLOGY
Pasadena, California

HYPERSONIC RESEARCH PROJECT

Memorandum No. 63

September 15, 1961

HOT-WIRE MEASUREMENTS IN
LOW REYNOLDS NUMBER HYPERSONIC FLOWS

by

C. Forbes Dewey, Jr.


Clark B. Millikan, Director
Guggenheim Aeronautical Laboratory

ACKNOWLEDGMENTS

The author would like to express his deep gratitude to Professor Lester Lees for suggesting this investigation and supervising the research program. Dr. Anthony Demetriades contributed greatly to the investigation in many ways; his hot-wire experience and assistance in obtaining the wake data were invaluable. Professor Toshi Kubota and Professor Edward Zukoski contributed many important suggestions and criticisms to the research program. The author wishes to thank Paul Baloga and the hypersonic staff for their many hours of expert assistance, Mrs. Geraldine Van Gieson for her help in preparing the manuscript, and Mrs. Truus van Harreveld for performing part of the computations. The cooperation of Dr. John Laufer and Dr. Thomas Vrebalovich of the Jet Propulsion Laboratory is also gratefully acknowledged.

A preliminary report on this work was presented to the American Rocket Society Annual Meeting, Washington, D. C., December 5-8, 1960.

ABSTRACT

Measurements were made of the heat loss and recovery temperature of a fine hot-wire at a nominal Mach number of 5.8. Data were obtained over an eight-fold range of Reynolds numbers in the transitional regime between continuum and free-molecule flow. At high Reynolds numbers, the heat transfer data agree well with the results of Laufer and McClellan, which were obtained at lower Mach numbers. At lower Reynolds numbers, the results indicate a monotonic transition between continuum and free molecule heat transfer laws. The slope of the heat transfer correlation also appears to vary monotonically, with $Nu \sim \sqrt{Re}$ at high Reynolds numbers and $Nu \sim Re$ for $Re < 1$.

Data on the wire recovery temperature (corresponding to zero net heat transfer) were obtained for free-stream Knudsen numbers between 0.4 and 3.0. Comparison with previous data suggests that for Mach numbers greater than about two the normalized variation of recovery temperature in the transitional regime is a unique function of the free-stream Knudsen number.

The steady-state hot-wire may be used to obtain two thermodynamic measurements: the rate of heat transfer from the wire and the wire recovery temperature. An illustrative experiment was performed in the wake of a transverse cylinder, using both hot-wire and pressure instruments in a redundant system of measurements. It was shown that good accuracy may be obtained with a hot-wire even when the Reynolds number based on wire diameter is small.

TABLE OF CONTENTS

PART	PAGE
Acknowledgments	ii
Abstract	iii
Table of Contents	iv
List of Figures	v
List of Symbols	vi
I. Introduction	1
II. Experimental Method	4
II. 1. Equipment	4
II. 2. Measurements	6
II. 3. Wire Calibration and Annealing	7
III. Data Reduction	11
IV. Results and Discussion	21
IV. 1. Heat Transfer Measurements	21
IV. 2. Recovery Temperature Measurements	28
V. Application of the Steady-State Hot-Wire to Wake Measurements	30
References	33
Appendix A -- End Loss Corrections for the Transitional Regime	36
Appendix B -- Measurement of the Wire Support Temperature	45
Appendix C -- The Effect of Overheat on Nusselt Number	48
Appendix D -- Measurements at Reynolds Numbers Approaching Free-Molecule Flow	52
Figures	53

LIST OF FIGURES

NUMBER		PAGE
1	Variation of Free Stream Mach Number with Tunnel Pressure	53
2	Variation of Stagnation Temperature with Tunnel Pressure	54
3	Hot-Wire Probe and Tunnel Installation	55
4	Typical Hot-Wire After Tunnel Exposure	56
5	Diagram of Calibration Oven	57
6	Electrical Circuit Diagram	58
7	Empirical Correlation of Hot-Wire Heat Transfer at Low Reynolds Numbers	59
8	Nusselt Number-Reynolds Number Relation for Supersonic and Hypersonic Flow	60
9	Slope of Nusselt Number-Reynolds Number Relation as a Function of Reynolds Number	61
10	Normalized Variation of Recovery Temperature with Knudsen Number	62
11	Data Obtained from Cylinder Wake Traverse	63
12	Variation of Flow Quantities Across the Cylinder Wake	64, 65
13	End Loss Relations for Nusselt Number Correction	66
14	End Loss Relations for Recovery Temperature Correction	67
15	Wire Support Temperature as a Function of Tunnel Pressure	68
16	Variation of Nusselt Number with Overheat	69
17	Nusselt Number-Reynolds Number Relation Approaching Free-Molecule Flow	70

LIST OF SYMBOLS

c_p	specific heat
d	hot-wire diameter
D	cylinder diameter
f	denotes a functional relation between two quantities
$f(s_1), g(s_1)$	functions of the molecular speed ratio s_1
h	convective heat transfer coefficient, $\frac{q}{T_w - T_{aw}}$
i	wire current
k	air thermal conductivity
k_w	wire thermal conductivity at temperature T_w
Kn	Knudsen number, $\sqrt{\pi \delta / 2} \quad (M/Re_\infty)$
l	wire length
M	Mach number
n	exponent in $Nu_o - Re_o$ relation: $Nu_o \sim Re_o^n$
Nu_m	Nusselt number measured with finite length wire, $h_m d/k_o$
Nu_o	Nusselt number for infinite length wire, hd/k_o
p	static pressure
P_{t2}	pitot pressure
Pr_o	Prandtl number, $c_p \mu_o / k_o$
q	heat transfer rate per unit area
R	wire resistance
Re	Reynolds number, $\frac{\rho_\infty U_\infty d}{\mu}$

s	resistance parameter, $\frac{\alpha_r T_o}{1 + \alpha_r (T_{awm} - T_r)}$
s_1	molecular speed ratio $\sqrt{\gamma/2} M$
t	non-dimensional temperature, $\frac{T - T_{awm}}{T_o}$
T	temperature
U_∞	free-stream velocity
v	support temperature parameter, (Eq. 12)
x	distance from cylinder axis in streamwise direction
y	distance from cylinder axis in transverse direction
a	accommodation coefficient
α_r	temperature-resistivity coefficient, $R_w/R_r = 1 + \alpha_r (T_w - T_r)$
γ	ratio of specific heats
δ^*	boundary layer displacement thickness
ϵ	recovery ratio parameter, $\eta_* - \eta_m$
ζ	end loss correction parameter, (Eq. 11)
η_c	experimental recovery ratio for continuum flow
η_f	theoretical recovery ratio for free molecule flow
η_m	measured recovery ratio, (T_{awm}/T_o)
η_s	non-dimensional support temperature, (T_s/T_o)
η_*	recovery ratio for infinite length wire, (T_*/T_o)
$\bar{\eta}$	normalized recovery ratio, $(\eta - \eta_c) / (\eta_f - \eta_c)$
μ	viscosity; also $(2/\sqrt{\pi}) (1/Kn) \log (1/Kn)$ in near free molecule flow analysis
ν	dimensionless quantity, (Eq. A-17)

ξ	measure of Nusselt number change with overheat, (Eq. A-19)
ρ	density
τ	overheat, $(T_w - T_{aw}) / T_{aw}$
χ	dimensionless quantity in near free molecule flow analysis, (Eq. 19)
ψ	dimensionless quantity in near free molecule flow analysis, (Eq. 20)
Ψ	end loss correction factor, (Eqs. 2 and 3)
ω	abbreviation for $(\tanh \nu / \nu)$

Subscripts

$()_{aw}$	zero current
$()_m$	measured
$()_o$	evaluated at stagnation temperature
$()_r$	evaluated at reference temperature T_r
$()_s$	evaluated at support temperature T_s
$()_w$	evaluated at wire temperature T_w
$()_*$	refers to infinitely long wire
$()_\infty$	free stream
$()_2$	behind a normal shock
$()_t$	evaluated at wake centerline

Superscripts

(\sim)	evaluated at zero overheat
$()'$	local value at edge of wake mixing region
$()^{(n)}$	the n^{th} approximation of an iterative solution
$(\overline{\quad})$	length-average or normalized quantity

I. INTRODUCTION

Hot-wire probes have been used for a number of years to measure the mean properties of a fluid stream. The hot-wire is capable of providing two thermodynamic measurements: the rate at which heat is transferred from the wire to the stream and the wire recovery temperature for zero heat transfer. If sufficiently accurate relations are known for the heat loss and recovery temperature as a function of the properties of the flow, only one additional thermodynamic measurement is necessary to specify the flow field uniquely.

The present investigation was undertaken with two purposes in mind. First, in using the hot-wire to measure mean quantities in low density compressible flow, it is necessary to have an accurate calibration of the wire heat loss and recovery temperature as a function of Mach number and Reynolds number. For high Reynolds number flows, these relations are well represented by the data of Laufer and McClellan¹. * Often, however, it is necessary to use the hot-wire in regions where the Reynolds number based on wire diameter is small. Previous investigations^{3, 4, 6, 7} have illustrated the general qualitative features of the $Nu - Re$ relation at small Reynolds numbers, but the experimental uncertainties are too large for calibration purposes. The first objective, therefore, was to obtain an accurate hot-wire calibration at high Mach number in the transition regime between continuum and free molecule flow.

* Superscripts denote references at the end of the text.

The second purpose of this investigation was to provide further information on two features of low Reynolds number flow which are important from a theoretical point of view. One of these is the recovery temperature phenomenon which was theoretically and experimentally investigated by Stalder, Goodwin, and Creager⁸. It was found by these authors that the equilibrium, or recovery, temperature of an unheated cylinder in free-molecule flow is greater than the stagnation temperature of the stream. Since the high Reynolds number equilibrium temperature is less than stagnation, the recovery ratio (T_{aw}/T_o) serves as one measure of the transition from continuum to free molecule flow. In the present investigation, measurements were made of the wire recovery temperature in the range of Knudsen numbers between 0.4 and 3.0. These and previous^{1, 2} data provide an accurate high Mach number relation between the recovery ratio (T_{aw}/T_o) and Kn over the complete range from continuum to free molecule flow.

At high Reynolds numbers, the heat transfer to the stagnation point of a blunt body may be accurately predicted using boundary layer theory. Recently, a considerable amount of attention has been given to the problem of determining appropriate corrections to the high Reynolds number, high Mach number boundary layer solutions which would extend their validity to lower Reynolds numbers. Several alternative formulations of this problem have been given in the literature, and more experimental evidence is needed to evaluate the results. The data obtained in this investigation, when combined with the results of Laufer and McClellan, show the departure of the Nu-Re relation from the high Reynolds number correlation and the approach to free-molecule flow for an infinite, conducting cylinder.

In many physical situations, it is difficult to obtain precise data using standard pitot probes. Particularly in regions of low density, instrumentation sufficiently large to obtain reliable results may introduce appreciable disturbances into the flow. Total temperature, mass flow, and velocity profiles in the wake of a transverse cylinder are reported here to illustrate the use of the hot-wire in such regions. By using both hot-wire and pressure measurements, the flow field was over-determined, and this redundancy permitted an estimate of the accuracy of the hot-wire measurements.

II. EXPERIMENTAL METHOD

II. 1. Equipment

The measurements were performed in Leg 1 of the GALCIT hypersonic wind tunnel at a nominal Mach number of 5.8. This tunnel has a 3 in. by 3 in. core of uniform flow. Other features of this facility are described in Reference 9. The stagnation pressure was varied between 0 and 95 psig. at a nominal stagnation temperature of 226°F. Because of the tunnel wall boundary layer, the actual test section Mach number varied with stagnation pressure as shown in Figure 1. Figure 2 shows the variation of stagnation temperature with pressure which was introduced by the automatic temperature regulation system.

Under certain conditions, free-stream turbulence may effect the measured heat transfer rate. Demetriades¹⁰ found that the free-stream integrated r. m. s. mass-flux and temperature fluctuations in Leg 1 were on the order of 0.4 per cent. The dominant turbulence scale, given by the velocity divided by the frequency, was on the order of 10^3 to 10^5 times the wire diameter, and by the criteria of Reference 12 should have caused no measurable effect on the heat loss. Additional quantitative turbulence measurements are necessary before a similar statement can be made about the wake results.

To determine the local Mach number, pitot pressure measurements were made within 0.5 in. of the hot-wire with the .063" I. D. stainless steel probe shown in Figure 3, and the local Mach number computed assuming isentropic flow between the reservoir and test section. The stagnation pressure was measured by a total head tube directly upstream of the throat. Traverses normal to the flow direction showed that the

local Mach number at the wire was identical to that measured by the probe within 0.5 per cent.

Stagnation temperatures were measured 1 inch ahead of the nozzle throat with a Pratt and Whitney type iron-constantan thermocouple, and all computations were made assuming isentropic, adiabatic expansion to the measured test Mach number.

The detachable hot-wire holders consisted of a conical brass body, a thin double wedge brass support blade, and two sewing needles to hold the wire. The needles were attached to and electrically insulated from the brass blade by epoxy resin; Figure 3a illustrates the holder configuration. The complete hot-wire assembly, including holder, sting support, and total pressure tube is shown in Figure 3b. The hot-wire was soft-soldered to the needle supports within .002" of the tips; a typical installation is shown in Figure 4. Details of the electrical connectors and head assembly may be found in Reference 10.

Figure 5 is a drawing of the calibration oven used to determine the temperature-resistance relation of the wires. Heat was supplied by a helically wound nichrome ribbon, and sufficient thermal lagging was used to make the temperature gradients within the oven negligible. An iron-constantan thermocouple placed 0.25 inch from the wire gave the oven temperature. Measurements were made only when the oven had reached thermal equilibrium (temperature change less than 0.2°F per minute).

The electrical instrumentation consisted of a precision Leeds and Northrup "K-2" potentiometer accurate to one part in 5,000, five-45 volt dry cells to supply the wire current, a variable series resistance for current control, and an auxiliary milliammeter and bridge as shown

in Figure 6. Measurements of the potential drop across the wire and the standard one ohm resistor were made with the K-2 potentiometer, giving the wire current and resistance. All readings were corrected for the small line resistance between the hot-wire and the potentiometer. During each series of measurements, the current was constant within 0.02 per cent.

II. 2. Measurements

To determine the Nusselt number and recovery temperature of the wire, the voltage drop across the wire and across a standard 1 ohm resistor were measured for several values of wire current. The resistance was then plotted against i^2 to determine the slope and intercept at zero current. Extreme care had to be exercised in achieving constant tunnel stagnation temperature, since a change of 1°F was easily detectable in the R vs. i^2 plot.

In performing the wake test, a continuous curve of wire temperature vs. position in the wake is desired for a fixed wire current, and a Mosely Autograph x-y plotter was used for this purpose. The traverse mechanism was geared to a linear resistance coil, and a small constant current through this resistance created a voltage drop proportional to the traverse position. This signal and the voltage drop across the hot-wire were the two electrical inputs for the plotter. Scale factors were obtained by measuring the voltage drop across the wire with the K-2 potentiometer at two known values of (y/D) .

II. 3. Wire Calibration and Annealing

The resistance of each wire was measured at several temperatures in the calibration oven. At the end of each series of runs, the wire resistance at room temperature was again measured; if the resistance had changed more than a few tenths of a per cent, the data were discarded. Several wires were calibrated both before and after prolonged testing to determine the effect of annealing and exposure on the temperature-resistivity coefficient.

All data were obtained using 0.00010 inch diameter Pt - 10 per cent Rh wire from a single spool. (Some preliminary tests using 0.00005 inch diameter wire are discussed in Appendix D.) No attempt was made to measure the wire diameter directly, since it was felt that the manufacturer's* drawing procedures were of greater accuracy than any available optical measurement technique. However, each wire was examined visually under a microscope to detect any macroscopic irregularities. The mounted wire resistance and length were also carefully measured and checked against the manufacturers quoted resistance of 11,580 ohms/ft. at 68°F. The mean deviation of the unannealed, installed resistance from this reference value was less than 1 per cent, indicating high uniformity of the wire.

Through prolonged use, the wire resistance increased between 2 and 8 per cent. Since it was necessary to limit the increase between successive calibrations to a few tenths of a per cent, several special tests were conducted to determine the major factors involved. It was found that a large part of the resistance shift could be eliminated by

* Sigmund Cohn, Mt. Vernon, New York.

heating the wire to a dull glow for several minutes prior to tunnel use. This result is in substantial agreement with the experience of Spangenberg (c.f., Reference 18, Figure 9). To check the influence of starting loads, one wire ($\frac{l}{d} = 325$) was subjected to seven consecutive tunnel starting cycles at 20 psig while immersed deep within the sidewall boundary layer. The resulting resistance change was less than 0.1 per cent.

It can be inferred that the primary causes of resistance change are associated with exposure to the free-stream pressure loads while the wire is at an elevated temperature. Further observation showed that the two primary factors were: (1) large step-wise increases in resistance if the previous maximum temperature and pressure of operation were exceeded ["deformation" phenomenon] ; (2) a much smaller increase which was a function of time ["creep" phenomenon] . Since all wires were initially normal to the flow direction, a certain amount of stretching was to be expected. Figure 4 shows a typical deformation caused by an overheat of about 0.8 at 90 psig stagnation pressure. Higher overheats resulted in larger wire curvature and were not used in this investigation. The creep phenomenon was negligible after the first few hours of tunnel exposure.

Two factors limited the aspect ratio of the wires. First, it was found that wire curvature increased with aspect ratio. Second, for aspect ratios greater than 375, wires of 0.00010" diameter were easily broken during the tunnel starting process. Since it was desired to keep the end loss corrections as low as possible, the range $320 \leq \frac{l}{d} \leq 360$ was chosen as an acceptable compromise.

The temperature coefficient of resistivity α_r varied between 0.88

and $0.93 (^{\circ}\text{F})^{-1}$ at 0°F , with a mean value of 0.91. Equilibrium wire temperatures were less than 270°F , and resistance varies linearly with temperature in this range. Calibration data were taken between 72 and 200°F , and the measured resistivity coefficient α_r was accurate to about 1.5 per cent for each wire. Several tests indicated that the resistivity coefficient was not affected by tunnel exposure, provided that the wire had been initially annealed to a dull glow in still air.

Under certain conditions, reversible strain gage effects may introduce systematic errors into the equilibrium temperature measurements. Using the relations of Morkovin (Reference 11, p. 24), the resistance error ΔR_w for this experiment caused by strain gage effects would be $(\Delta R_w/R_w) \sim 10^{-4}$ to 10^{-5} , or considerably less than the uncertainty of the wire calibration. A more serious error could be introduced by differential thermal expansion between the wire and the support head. However, no evidence of this effect was present in the temperature calibrations, and since tunnel operation was less severe from this standpoint than the oven calibration, it was assumed that thermal strain was negligible.

In Appendix A, the correction factors for heat loss to the wire supports are derived. This analysis is carried through with the support temperature as a free parameter, and shows that for large end loss correction the support temperature has an important effect on both the Nusselt number and recovery factor. Depending upon the tip shape, thermal conduction, and free-stream Reynolds number the effective value of $\eta_s = (T_s/T_o)$ should lie between .85 and 1.0, and should vary with the wire attachment location. Since the recovery temperature correction was quite sensitive to η_s , a special test (see Appendix B)

was conducted to measure this parameter. The value of η_s was found to be constant over the complete range of tunnel conditions encountered, and equal to $0.903 \pm .005$. This value is approximately equal to the calculated laminar boundary layer recovery factor for flow along the needle downstream of the stagnation region.

III. DATA REDUCTION

In previous hot-wire investigations, many attempts have been made to secure a universal correlation of Nusselt number as a function of Reynolds number and Mach number. Since hot-wire data have been obtained in several different gases over a Reynolds number range of eight orders of magnitude, for Mach numbers between zero and six and for wire overheats τ between 0 and 2, it is by no means a trivial matter to find correlations which represent the data over any large range of parameters.

The largest portion of heat transferred from a blunt body is in the vicinity of the forward stagnation point. At high Reynolds numbers and Mach numbers, the appropriate temperature for evaluating viscosity and thermal conductivity is that existing behind a normal shock at the free stream Mach number. At low Reynolds numbers, a distinct shock wave does not appear; under these conditions, the results of free molecule theory⁸ may be conveniently expressed using fluid properties evaluated at the stagnation temperature. At high Mach numbers, the temperature behind a normal shock is close to the stagnation temperature and the two evaluations will give equivalent, but not identical, correlations. In this paper, the heat transfer data are correlated using the Nusselt and Reynolds numbers

$$\text{Nu}_0 = (hd/k_0) \quad , \quad \text{Re}_0 = (\rho_\infty U_\infty d)/\mu_0 \quad , \quad (1)$$

where μ_0 and k_0 are the air viscosity and thermal conductivity evaluated at stagnation temperature. This form offers distinct advantages when the hot-wire is used as a measuring instrument in

non-uniform flow fields.*

All hot-wires of finite length lose a certain amount of heat to their supports. The quantity Nu_o represents the heat transfer rate for a wire of infinite length, and is related to the measured Nusselt number Nu_m by the relation

$$Nu_o = \Psi_N Nu_m = \Psi_N \left[\frac{i^2 R_m}{\pi l k_o (T_w - T_{awm})} \right] \quad (2)$$

where Ψ_N is the Nusselt number end loss correction factor, $i^2 R_m$ is the measured Joule heating, and $(T_w - T_{awm})$ is the measured temperature potential. Similarly, the recovery ratio η_* for an infinitely long wire may be written

$$\eta_* = (T_{aw*}/T_o) = \Psi_R \eta_m = \Psi_R (T_{awm}/T_o) \quad (3)$$

where Ψ_R is the recovery ratio end loss correction factor. In Appendix A, the quantities Ψ_N and Ψ_R are derived in detail. They depend primarily on the wire aspect ratio and measured Nusselt number; for large aspect ratios and Nusselt numbers, Ψ_N and Ψ_R are close to unity.

The present measurements were conducted using very small heating currents. For $i \rightarrow 0$ and a linear temperature - resistance relation,

$$\frac{i^2 R_m}{(T_w - T_{aw})} = a_r R_m R_r \left(\frac{i^2}{R_m - R_{awm}} \right) \approx \frac{a_r R_{awm} R_r}{(dR/di^2)_{i=0}}$$

and Eq. 2 takes the simplified form

* Morkovin¹¹ and Collis and Williams¹³ discuss this problem in more detail.

$$Nu_m = \left(\frac{a_r}{\pi \ell k_o} \right) \frac{R_{awm} R_r}{(dR/di^2)_{i=0}} \quad (2a)$$

A plot of R vs. i^2 (e. g. Figure 11) allows the quantity $(dR/di^2)_{i=0}$ to be determined accurately.

For high Reynolds numbers, the recovery ratio $\eta_c = (T_c/T_o)$ has been shown experimentally to be a function only of Mach number¹¹; η_c decreases from 1.0 at $M = 0$ to 0.95 for Mach numbers greater than about two. This behavior is explained by the well-known hypersonic "freeze" or Mach number independence principle, which recognizes that the viscous and inviscid flow fields become independent of Mach number if the Mach number is sufficiently large. For blunt bodies such as the cylindrical wire considered here, changes in the flow field are small beyond a Mach number of three.* A value $\eta_c = 0.950$ was used as a reference for the present experiments and the data of Laufer and McClellan¹ and Sherman². Stalder et al⁵ found $\eta_c = 0.96$, and this value was used in interpreting their results.

The high Reynolds number relations described above represent the limit of continuum flow. For free molecular flow, the heat loss and recovery temperature of an infinite, perfectly conducting cylinder with no radiative cooling are given in Reference 8:

* Tewfik and Geidt¹⁴ have measured the angular variation of heat transfer coefficient and recovery temperature for a cylinder at Mach numbers of 1.3 and 6.0. These distributions, which are similar to those obtained at low speeds, may be used to calculate the temperature T_{aw} which a cylinder of infinite thermal conductivity would assume for no net heat transfer. As expected, the resulting values of $T_{aw}(M)$ agree well with the hot-wire measurements.

$$Nu_o = \frac{(\delta - 1)}{2(\pi)^{3/2}} \propto Re_o \cdot Pr_o \left(\frac{g(s_1)}{s_1} \right) \quad (4)$$

$$\eta_f = (T_{aw}/T_o) = \left(1 + \frac{\delta - 1}{2} M^2 \right) \frac{f(s_1)}{g(s_1)} \quad (5)$$

$$s_1 = \sqrt{\delta/2} M \quad (6)$$

where $f(s_1)$ and $g(s_1)$ depend only on the molecular speed ratio s_1 and the number of excited degrees of freedom of the medium. These functions are tabulated in Reference 8 for both monatomic and diatomic perfect gases. As $M \rightarrow \infty$, Eqs. (4) and (5) approach the limiting forms

$$Nu_o = \left(\frac{\delta + 1}{2\pi\delta} \right) \propto Re_o \cdot Pr_o \quad (4a)$$

and

$$\eta_f = \left(\frac{2\delta}{\delta + 1} \right) \quad (5a)$$

As in the case of continuum flow, the Nusselt number and recovery ratio become independent of Mach number as the Mach number increases.*

The fact that the recovery ratio in continuum and free molecule flow obeys the Mach number independence principle suggests that the normalized recovery ratio

$$\bar{\eta}_* = \frac{\eta_* - \eta_c}{\eta_f - \eta_c} \quad (7)$$

is a unique function of the Knudsen number for M sufficiently large. At lower Mach numbers, $\bar{\eta}_*$ would depend on additional parameters involving M and Re . Cybulski and Baldwin⁷ report that for subsonic flow the continuum recovery ratio persists to quite high Knudsen numbers.

* Reference 15 gives several additional examples of the Mach number independence principle for both continuum and free molecule flow.

All computations of flow properties were made using $\delta = (7/5)$ and the Sutherland viscosity formula (with T expressed in $^{\circ}\text{R}$)

$$\mu = 2.270 \frac{T^{3/2}}{198.6 + T} \times 10^{-8} \text{ , } \frac{\text{lb} \cdot \text{sec}}{\text{ft}^2} \quad (8)$$

Values of air thermal conductivity were obtained from Hilsenrath and Beckett¹⁶, and the wire thermal conductivity was taken from Reference 17, with the data linearly extrapolated to the measured mean wire temperature.

A derivation of the end loss corrections appropriate to transitional flow is given in Appendix A. This analysis assumes that the wire temperature is radially uniform, wire resistance is a linear function of temperature, and the heat transfer coefficient $h = \text{Nu}_0 (k_0/d)$ is constant over the wire length. For convenience, the supports are taken to be equal in temperature, although this restriction is not essential. The relation between the measured Nusselt number Nu_m and the value Nu_0 for an infinite wire may be expressed as

$$\Psi_N = \left(\frac{\bar{t}}{t_* - \epsilon} \right) \frac{(1 + st_*)}{(1 + s\bar{t})} \quad (9)$$

while the recovery ratio end loss correction factor is given by

$$\Psi_R = \frac{\eta_*}{\eta_m} = \left[1 - \tilde{\omega} \left(\frac{\eta_s}{\eta_m} \right) \right] (1 - \tilde{\omega})^{-1} \quad (10)$$

Here η_s is the normalized support temperature, η_m is the measured recovery ratio, $s\bar{t}$ and st_* represent normalized resistances, and $\tilde{\omega}$ is a parameter which depends primarily on the wire aspect ratio and Nusselt number; $\tilde{\omega}$ represents the zero overheat value of ω . The quantities $[\bar{t}/(t_* - \epsilon)]$ and $[\omega/(1 - \omega)]$ are given in Figures 13 and 14 as functions of the two parameters

$$\zeta = (\ell/d) \left[(k_o/k_w) \text{Nu}_m \frac{(1 + \epsilon s)}{(1 + s \bar{t})} \right]^{\frac{1}{2}} \quad (11)$$

and

$$v = -\frac{1}{2} t_s s (\tilde{\omega}/\omega) \frac{(1 - \omega)}{(1 - \tilde{\omega})} \quad (12)$$

It is shown in Appendix A that the correction factor $\bar{\Psi}_N$ does not depend strongly on overheat; for $\tau \longrightarrow 0$, Eqs. (9) - (12) assume the more tractable form

$$\bar{\Psi}_N = \left(\frac{\bar{t}}{t_* + \epsilon} \right) (1 + \epsilon s) \quad (9a)$$

$$\bar{\Psi}_R = 1 + \left(1 - \frac{\eta_s}{\eta_m} \right) \left(\frac{\omega}{1 - \omega} \right) \quad (10a)$$

$$\zeta = (\ell/d) \left[(k_o/k_w) \text{Nu}_m (1 + \epsilon s) \right]^{\frac{1}{2}} \quad (11a)$$

$$v = -\frac{1}{2} t_s s \quad (12a)$$

where

$$\epsilon = (\eta_* - \eta_m) \ll 1$$

$$t_s = (\eta_s - \eta_m) \ll 1$$

and s is a constant of order one. As ζ decreases, both $\bar{\Psi}_N$ and $\bar{\Psi}_R$ depart from unity; the support temperature parameter v plays a minor role in determining the end loss corrections, although it must be considered if the corrections are large.

These corrections were applied to the present data and to the recovery factor data of Laufer and McClellan¹ at the lower Reynolds numbers of their investigation. As discussed in the following section, this correction was primarily responsible for unifying the results of the several investigations of recovery temperature in supersonic flow.

For the present data, the measured value $\eta_s = 0.903$ was used with the measured values of η_m and Nu_m to compute the end loss correction. A slightly more complicated procedure was required in interpreting the results of Laufer and McClellan¹. In that investigation, measurements of the Nusselt number and recovery factor were made with different wires; the Nu_o data were obtained with wires of aspect ratio between 400 and 550 and the recovery temperature data were obtained using aspect ratios of the order of 225. The Nusselt numbers reported in Reference 1 include a small (less than 5 per cent) end loss correction; for such small corrections the formulas used are essentially identical to those derived in Appendix A. The data given in Reference 1, therefore, represent Nu_o in the present nomenclature (the actual parameters used by Laufer and McClellan¹ were Nu_2 and Re_2 ; conversion to Nu_o and Re_o is obvious). The reported recovery ratio, however, represents η_m and requires a correction to account for support conduction.

The wire supports used by Laufer and McClellan¹ were equivalent to a two-dimensional wedge of 7° included angle. Using the observation (Appendix B) that the support temperature is equal to the laminar boundary layer adiabatic wall temperature, η_s could be calculated explicitly. Since Nu_m was not known, an iterative computation process was adopted which used as input the known quantities η_s , η_m and the wire Reynolds number Re_o . With Re_o known, Nu_o was taken from the heat loss correlation and the value of Nu_m was computed. The procedure for obtaining Nu_m and η_* with Nu_o and η_m known is analogous to the determination of Nu_o and η_* with Nu_m and η_m given.

The present free stream data were subject to end loss corrections in the ranges $.703 \leq \Psi_N \leq .833$ and $1.208 \leq \bar{\Psi}_R \leq 1.633$.

For the low Reynolds number wake tests, values $.59 \leq \overline{\Psi}_N \leq .68$ and $1.70 \leq \overline{\Psi}_R \leq 2.06$ were used. In view of the appreciable end losses encountered, it should be emphasized that the important thing is not the magnitude of the corrections per se, but the accuracy with which these corrections are known. The largest uncertainty lies in the actual end conditions of the wire, as characterized by η_s ; for this reason, η_s was measured directly in the present investigation (Appendix B). This parameter is sensitive not only to the shape and material properties of the support but also to the flow field around the tips. In transonic or non-uniform flow fields, the determination of an effective value of η_s is a formidable problem, as Sherman² has pointed out.

No correction was made to the data for radiation effects since calculation showed that the error in both Nu_0 and \overline{h}_* was less than one tenth of one per cent. The correction is roughly proportional to (T_w^4/Nu) , and may become appreciable for high overheats or extremely low Reynolds numbers.

The raw data from the wake traverse consisted of a series of continuous curves of wire voltage vs. voltage output from the traverse mechanism. The voltage scale was established by two calibration measurements with the K-2 potentiometer at known values of (y/D) . Using this calibration and the measured value of wire current, the wire resistance was computed for several representative stations within the wake. Figure 11 shows the measured wire resistance as a function of wire current.

Two thermodynamic measurements were obtained with the hot-wire; these were $[dR/d(i^2)]_{i=0}$ and the zero current intercept R_{aw} , both of which were taken from Figure 11. Pitot pressure and static

pressure across the wake were also measured separately. Thus, the measured thermodynamic quantities were more than sufficient to specify the flow completely, and this redundancy permitted an estimate of the accuracy of the combined measurements. A description of the computation procedure is given below.

From the four quantities $[dR/d(i^2)]_{i=0}$ (i. e., Nu_m), R_{aw} (i. e., T_{aw}), p_{t2} , and p , four groups of three independent quantities may be formed, and any one of these groups would provide sufficient data to determine the state of the flow uniquely. Any two groups would provide an independent, redundant calculation; in certain cases, the accuracy and convergence of the iterative solution may depend strongly on the choice of parameters.* For purposes of illustration, the following groups of variables were chosen**:

$$\text{Group I: } [dR/di^2]_{i=0}, R_{awm}, p$$

$$\text{Group II: } p_{t2}, R_{awm}, p$$

The computation procedure is similar in principle to that which would be used for any two groups of three variables.

To interpret the local values $[dR/di^2]_{i=0}$ in the wake an empirical relation between Nu_0 and Re_0 was required for the range $.34 < Re_0 < .66$, only part of which was covered by the present free-stream measurements. For the lower Reynolds numbers, the calibration curve given in Figure 8 was extrapolated to $Re_0 = .315$ using a smooth

* Several examples are cited by Morkovin¹¹ to illustrate this point.

** Quantities without superscripts are functions of distance from the wake centerline, while ()' signifies the measured value at the edge of the wake mixing region.

curve which asymptotically approached the free molecule heat transfer law [Eq. (4)] , with $\alpha = 1.0$. The justification for this choice of α is given in the following section. Interpretation of the measured recovery temperature was made using values of $\bar{n}_* (Kn)$ given by the solid curve of Figure 10.

The static and pitot pressure measurements were obtained by John F. McCarthy, Jr. of this laboratory. Free stream conditions for the hot-wire and pressure traverses were

	$\frac{M_\infty}{}$	$\frac{x/D}{}$	$\frac{Re_{\infty, D}}{}$
Hot-wire	5.74	9.0	1.75×10^4
Pressure	5.74	9.0	2.60×10^4 .

Hot-wire fluctuation measurements showed that the wake was laminar in both cases, and the assumption was made that the local pressure profiles were similar for the two tests. The Reynolds number effect is discussed more fully in Section V.

Data reduction was most conveniently carried out by assuming distributions of the unknown flow quantities across the wake, computing the end loss corrections based on these assumed values, and from the measured quantities and the end loss corrections obtaining improved guesses for the unknown quantities. For Group I, this iteration was performed using M and T_0 as the unknowns; the calculation for Group II used T_0 as the iterative quantity. In both cases, only three iterations were required to obtain convergence.

IV. RESULTS AND DISCUSSION

IV. 1. Heat Transfer Measurements

In attempting to compile an empirical correlation of hot-wire heat transfer data over an extended range of variables, the investigator is faced with two problems: the number of experimental papers on the subject is quite large, running well over fifty, and the results of investigations conducted under seemingly identical conditions differ by as much as 40 per cent. The effects of wire overheat and stagnation temperature (particularly in the transonic regime) have yet to be fully resolved.¹⁹

Figure 7 has been prepared as a guide to the experimental variation of Nusselt number as a function of Reynolds number and Mach number in the range $0.2 \leq Re_0 \leq 100$. In preparing the figure particular weight was given to the correlation of McAdams²⁰ at $M = 0$ and the results of Laufer and McClellan¹ and the present investigation at Mach numbers greater than two. Within the Reynolds number range $1 \leq Re_0 \leq 100$, the data of Baldwin²¹ and Cybulski and Baldwin⁷ are representative of the information available at subsonic velocity. Spangenberg's data (Reference 19, Figure 17c) show a similar Mach number variation for Reynolds Numbers greater than one, and far better agreement with References 1 and 20 than the work of Baldwin. The cold wire data of Christiansen²² at low Reynolds numbers are also included. These transonic measurements agree well with the hot-wire results for $Re_0 < 1$, and provide a consistent set of measurements in the near free molecule flow regime. At low Reynolds numbers, the correlation would be changed considerably if incomplete accommodation were present.

Theoretical studies are of limited use in preparing a heat transfer

correlation. The solution of Cole and Roshko²³ for continuum Oseen flow agrees well with the experiments of Collis and Williams²⁴ at low Reynolds numbers. Levy²⁵ has considered the Oseen flow problem with temperature-jump boundary conditions, and the results agree qualitatively with the experiments of Cybulski and Baldwin⁷. However, the velocities and Reynolds numbers covered by Oseen theory are quite small.

Free molecule analysis has provided what appears from Eq. (4) to be a straightforward calibration for all flows where the Knudsen number is sufficiently high. The fact that the accommodation coefficient α is an arbitrary parameter has been a major weakness in all attempts to apply this theory to a given set of data.* It is not uncommon to find investigations with an experimental scatter greater than 30 per cent in which the authors infer a specific value of accommodation coefficient by comparing the asymptotic behavior of their $Nu_o - Re_o$ curve to Eq. (4), and ascribing the difference to incomplete accommodation.

The heat transfer data obtained in this investigation are presented in Figure 8. These data agree well with the measurements of Laufer and McClellan¹ at Reynolds numbers Re_o greater than three. One may infer from this agreement and the Mach number independence principle that the solid line shown in Figure 8 represents the $Nu_o - Re_o$ relation for Mach numbers greater than about two.

For comparative purposes, the results of free molecule theory [Eq. (4)] and the extrapolated slope of the high Reynolds number data are shown in Figure 8. At high Reynolds numbers, the Nusselt number becomes proportional to $(Re_o)^{\frac{1}{2}}$, while $Nu_o \sim Re_o$ for $Re_o \ll 1$. The

* An excellent appraisal of the problems of momentum and energy accommodation is given by Hurlbut²⁶.

present measurements asymptotically approach the free molecule result with an accommodation coefficient α near unity. For the heat transfer tests in air and argon by Christiansen²³, Weltman and Kuhns⁶, and Wong³, an accommodation coefficient of unity represents the data within the experimental error. Experimentally, it has been found that surface conditions are of primary importance in determining the degree of energy accommodation²⁶; the presence of adsorbed gases on the body surface increases the accommodation coefficient.

All data shown in Figure 8 are based on the measured Nusselt number at zero overheat; however, the effects of overheat are discussed in detail in Appendix C. In free molecule flow, the surface temperature enters the heat transfer relation only through its effect on the accommodation coefficient. If the accommodation coefficient were unaffected by surface temperature, the cold wire results of Christiansen²² and the present results should agree closely [except for the small Mach number variation given by $f(s_1)/s_1$ in Eq. (4)]. Figure 7 indicates that the hot wire and cold wire data agree well up to a Reynolds number Re_o of about one.

For high Reynolds number flows, a large part of the heat transfer to the body occurs in the vicinity of the forward stagnation point. For a perfect gas, the heat transfer at the stagnation point of a cylinder in supersonic flow is closely represented by²⁷

$$Nu_o \cong 0.50 \sqrt{Re_o} \left(\frac{Pr_o}{Pr_w} \right) \left(\frac{T_o}{T_w} \frac{\mu_w}{\mu_o} \right)^{.06} \quad (13)$$

Equation (13) indicates that the effects of overheat at high Reynolds numbers should be small over the range of conditions encountered in the laboratory.

Although no complete solutions are available for a cylinder in high speed flow because of the lack of an adequate theory covering the region of separation, many analyses are available for heat transfer near the stagnation point of a blunt body. It has been pointed out that both the hot-wire data and the stagnation point boundary layer solutions exhibit heat transfer coefficients proportional to $\sqrt{\text{Re}_0}$ at high Reynolds numbers, and the behavior of the stagnation point solutions with decreasing Reynolds number should agree well with the hot wire measurements.

Two recent investigations by Probstein and Kemp²⁶ and Van Dyke³² have used the Navier-Stokes equations to describe the flow field near the stagnation point of a blunt body in hypersonic flow. These analyses show that conventional high Reynolds number boundary layer theory must be modified as the body Reynolds number is decreased. First order corrections may be present due to external vorticity, boundary layer displacement, surface velocity and temperature jump, and body curvature. For a cylinder, the vorticity along the zero streamline is zero in the inviscid flow, so the vorticity effect on heat transfer is of second order. However, the boundary layer displacement and curvature effects both produce a first order decrease in surface heat transfer, compared with the conventional high Reynolds number value. Slip effects would also decrease the heat transfer rate. Probstein and Kemp²⁶ have proposed a merged layer analysis based on continuum relations for the range $30 \lesssim \text{Re}_0 \lesssim 100$. The results agree qualitatively with the present measurements.

The slope of the $Nu_o - Re_o$ relation is a quantity of considerable interest. The exponent n in the relation

$$Nu_o \sim Re_o^n \quad (14)$$

correlates the results of several independent investigations better than the absolute magnitudes of the observed quantities. In Figure 9, the exponent n is shown as a function of Reynolds number and Mach number for several investigations. The present measurements and those of Laufer and McClellan¹ were used for $M > 2$, while selected results of Christiansen²², Cybulski⁷, and Baldwin²¹ are shown for $M < 1$. At high Reynolds numbers, the exponent n is $\frac{1}{2}$; in the limit of $Kn \rightarrow 0$, the free molecule relation, Eq. (4), shows that $n = 1$. A third relation, derived from the Oseen solution of Cole and Roshko²³, is applicable when $M/Re < < 1$ and $Re_o < < 1$; in this instance, the exponent is of the form

$$n = \frac{1}{\log \left(\frac{8}{Re_o Pr_o} \right)} \quad (15)$$

Collis and Williams²⁴ experiments agree very well with Eq. (15) for $0.01 < Re_o < 0.3$.

At high Mach numbers, the exponent n is seen to vary monotonically between the continuum and free molecule values of $\frac{1}{2}$ and 1. The measured slope begins to depart from the continuum value at a Reynolds number Re_o of about 200 for an insulated wire. A comparison between Christiansen's²² data and the present measurements indicate that the departure from the continuum heat transfer law occurs at a slightly lower value of Re_o if the wall is highly cooled; this may be explained by the fact that a cool wall decreases the boundary layer displacement effect at a given Reynolds number. For low Reynolds numbers, the

approach to the free molecule heat transfer law does not appear to vary with wire overheat, although the data are not sufficient to completely resolve this question.

Willis²⁹ has treated several problems in the near free molecule regime using an iterative solution to the integral form of the Boltzmann equation. This approach is equivalent to the so-called first collision theory if only the first iterate is considered. Willis' results for a two-dimensional strip normal to a rarefied flow should be identical in form to the solution for a cylinder normal to the flow. By writing a heat balance for the body, the resulting equations may be solved for the departure of the Nusselt number and recovery temperature from the free molecule values as a function of the free stream Knudsen number. The results may be expressed as ($\alpha = 1$)

$$\frac{Nu_o}{(Nu_o)_{\text{Free Molecule}}} = 1 + \mu \chi \quad (16)$$

$$\frac{T_{aw}}{(T_{aw})_{\text{Free Molecule}}} = \frac{1 + \mu \psi}{1 + \mu \chi} \quad (17)$$

where

$$\mu = \frac{2}{\gamma \pi} \frac{1}{Kn} \log\left(\frac{1}{Kn}\right) \quad (18)$$

$$\chi = \frac{N_i - N_{if}}{\mu N_{if}} \quad (19)$$

$$\psi = \frac{Q_i - Q_{if}}{\mu Q_{if}} \quad (20)$$

Here N_i is the incident molecular flux, Q_i is the incident energy flux, and $(\quad)_f$ indicates the value for $\mu \rightarrow 0$.

Willis has evaluated the parameters ψ and χ for a two-dimensional strip, and finds that they depend on the molecular speed ratio, the body temperature, the molecular model, and the number of degrees of freedom of the gas. ψ and χ are weak functions of the body temperature if the overheat is small; the results are more sensitive to body temperature at higher values of the molecular speed ratio s_1 . For $s_1 \rightarrow \infty$, Willis has computed ψ and χ as a function of body temperature for both the hard sphere and modified Krook molecular models. For an insulated body ($T_w = T_{aw}$), $\psi = .42$ and $\chi = .11$ for the modified Krook model while $\psi = .78$ and $\chi = .48$ if the hard sphere model is used. From Equation (16), it may be seen that the departure of the Nusselt number from the free molecule result is a strong function of the molecular model employed. Eqs. (16) and (17) agree qualitatively with the present experiments if $\psi > \chi > 0$.

Several interesting conclusions may be drawn from the above analysis. First, the small parameter in near free molecule flow for a two-dimensional body is $(1/Kn) \log (1/Kn)$ rather than the quantity $(1/Kn)$ which pertains to axisymmetric bodies. Thus, the range of validity of the two-dimensional analysis is restricted to higher Knudsen numbers than the axis-symmetric counterpart. Second, for viscosity proportional to $(T)^{\frac{1}{2}}$, $Kn \sim (1/Re_0)$ at high Mach number and the analysis predicts that the $Nu_0 - Re_0$ relation at high Knudsen numbers should, as expected, become independent of Mach number.

IV. 2. Recovery Temperature Measurements

Measurements of the recovery temperature of a cylinder placed normal to the flow have previously been made at high Reynolds numbers up to a Mach number of 4.5. The excellent work of Laufer and McClellan has shown that the recovery temperature is independent of Mach number above approximately 2. A justification of this effect has already been given.

In the transitional regime, the measurements reported in References 1 and 2 indicated that at Knudsen numbers of about 0.1 the recovery temperature begins to rise above the high Reynolds number value, while at Knudsen numbers greater than 10, the full temperature rise predicted by Eq. (5) is attained. However, at Knudsen numbers of about 1 and at roughly the same Mach number, the two investigations reported significant differences in the recovery factor.

The present investigation was undertaken in an attempt to resolve this apparent discrepancy and at the same time provide additional recovery temperature data for use in steady-state hot wire work. The results are shown in Figure 10, using the normalized recovery ratio $\bar{\eta}_*$ and the free-stream Knudsen number as parameters. Fortunately, the recovery temperature for a cylinder is independent of the accommodation coefficient (provided that the wire is infinitely long!) and rapidly approaches an asymptote as the Mach number increases. Therefore, since $\bar{\eta}_* = 0$ for $N_* = N_c$ and $\bar{\eta}_* = 1$ for $N_* = N_f$, all investigations should agree at least in these two limits.

The shaded area representing the data of Laufer and McClellan defines the limits of experimental scatter of nearly 100 separate measurements made over a large range of Mach and Reynolds numbers.

Considering the range of parameters studied, the data are extremely consistent. However, the aspect ratios of the wires used in their recovery temperature study were on the order of 200, and at the higher Knudsen numbers these wires were subject to significant end losses. Using the relations derived in Appendix A several representative data points were corrected for support conduction and plotted in Figure 10.

By combining the corrected data of Reference 1, the results of Sherman², and the present measurements, a continuous transition of the normalized recovery factor is obtained between continuum and free molecule flow. From a consideration of the Mach number independence principle, this curve should be valid for all Mach numbers above approximately two. Considering the sensitivity of the normalized recovery ratio to experimental error, the correlation appears to be very good. At lower Mach numbers, the $\bar{\eta}_*(Kn)$ correlation should show a dependence on Mach number.

The behavior of the $\bar{\eta}_*(Kn)$ relation at small Knudsen numbers agrees qualitatively with the results of Probstein and Kemp²⁸. In the incipient merged layer analysis, they find that the gas temperature at the stagnation point of a blunt body becomes greater than the free stream stagnation temperature in the low Reynolds number continuum range. For large Knudsen numbers, Eq. (17) predicts that the recovery temperature will fall below the free molecule value if $\psi > \chi$; the experimental data shown in Figure 10 indicate that for a circular cylinder and a diatomic gas, ψ and χ are nearly equal.

V. APPLICATION OF THE STEADY-STATE HOT-WIRE TO WAKE MEASUREMENTS

Several classic experiments have been made using the hot-wire as a steady-state measuring instrument. These have been well reported in the cited references, and it is pertinent only to emphasize that wire calibration is the primary problem in all quantitative measurements.

The number of investigations utilizing the hot-wire in a redundant measurement scheme is quite small, and consequently it was decided to perform an illustrative experiment involving four measured quantities, two of which were obtained from a hot-wire operated in the transitional regime. The wake of a cylinder transverse to a hypersonic flow was chosen both because its flow field was amenable to hot-wire and pressure measurements and because of current interest in the thermal wakes of hypersonic blunt bodies.

The wire used in this experiment had an aspect ratio of 311 and $\alpha_r = 0.93$. The measured variation of wire resistance with i^2 is shown in Figure 11. One important conclusion which can be drawn is that the instrument sensitivity was quite sufficient to pick out small differences in the R vs. i^2 relation. This property is absolutely essential for quantitative interpretation.

The following groups of variables were chosen to represent the data:*

$$\text{Group I:} \quad \left[\frac{dR}{d(i^2)} \right]_{i=0}, R_{awm}, p$$

$$\text{Group II:} \quad p_{t2}, p, R_{awm}.$$

* See Section III for a discussion of the data reduction procedure.

The distributions of flow quantities across the wake were computed using the measurements of Group I and Group II in independent calculations. Thus, the agreement between the results of Group I and Group II provides a measure of the accuracy of the combined measurements.

Figure 12a shows the results of the stagnation temperature calculation. T_o' is the measured stagnation temperature at the outer edge of the mixing layer. Results for the several representative stations are shown first as "uncorrected" data. By "uncorrected" is meant the temperature one would calculate using only the zero current intercept of Figure 11 and the wire resistivity coefficient. The wire was subject to end loss effects, and by using Figures 8 and 10 and the derived end loss corrections, an iteration was performed to find the true value of T_o . Only three iterations were required to obtain convergence.

Qualitatively, the behavior of (T_o/T_o') is similar to that obtained in a high speed boundary layer¹ with Prandtl number less than one. Because of laminar shear and heat conduction processes, the centerline Mach number for this particular streamwise station was about 3/4 of M' and the centerline stagnation temperature was about 0.96 of T_o' . The two values of T_o' agreed within 0.14 per cent, and were two per cent lower than the free stream stagnation temperature. This result agrees well with the postulate of isoenergetic flow everywhere outside the viscous mixing region.

The local mass flow in the wake is shown in Figure 12b. For purposes of comparison, the "uncorrected" hot-wire data is also shown; the measured heat loss of the wire $R_{aw} (dR/di^2)^{-1}$ is directly proportional to the local mass flow (ρu) if end losses are negligible. Since the end loss correction increases with decreasing (ρu), the uncorrected mass flow

is higher than the final corrected values based on the measurements of Group I.

The agreement between the two values of $(\rho u / \rho' u')$ computed using Group I and Group II is good. The differences between the two curves are primarily due to the different cylinder Reynolds numbers for the hot-wire and pressure tests (see page 20). Subsequent pitot pressure data have indicated that the higher value of $(\rho u / \rho' u')$ at the wake centerline obtained with Group II is caused by the higher values of $Re_{\infty, D}$ for the pressure measurements. At the edge of the wake, $(\rho' u')$ for Group I was 0.85 of $(\rho' u')$ for Group II. Taking this Reynolds number effect into account, the absolute values of (ρu) from Group I and Group II were found to agree within 7 per cent throughout the mixing region. The small differences between the two values of (T_o / T_o') shown in Figure 12a are also attributable to the difference in $Re_{\infty, D}$.

The velocity defect in the wake mixing region is shown in Figure 12c. The agreement between the hot-wire and pressure measurements is seen to be excellent, and verifies the fact that the differences shown in Figures 12a and 12b are due to differences in $Re_{\infty, D}$; for $(x/D) = 9$ and these Reynolds numbers, the wake is laminar and the velocity defect $[(u - u_{\infty}) / (u' - u_{\infty})]$ should show little dependence on $Re_{\infty, D}$.

In summary, this wake survey has shown that the steady-state hot-wire may be used as an accurate quantitative instrument when operated at small wire Reynolds numbers, provided sufficiently accurate calibration relations are available. The hot-wire is capable of providing two thermodynamic measurements; only one additional measurement (such as total or static pressure) is required to determine the flow field uniquely.

REFERENCES

1. Laufer, J. and McClellan, R., "Measurements of Heat Transfer from Fine Wires in Supersonic Flows", J. Fluid Mech., Vol. 1, No. 3, pp. 276-289, 1956.
2. Sherman, F. S., "A Low-Density Wind-Tunnel Study of Shock-Wave Structure and Relaxation Phenomena in Gases", NACA TN 3298, 1955.
3. Wong, Howard, "Design and Development of a Free-Molecule Heat Transfer Probe", U. of Calif. (Berkeley) Report HE-150-143, 1956.
4. Laurman, J. A. and Ipsen, D. C., "Use of a Free-Molecule Probe in High Speed Rarefied Gas Flow Studies", U. of Calif. (Berkeley) Report HE-150-146, 1957.
5. Stalder, J. R., Goodwin, G., and Creager, M. O., "Heat Transfer to Bodies in a High-Speed Rarefied-Gas Stream", NACA Report 1093, 1952.
6. Weltmann, R. N. and Kuhns, P. W., "Heat Transfer to Cylinders in Crossflow in Hypersonic Rarefied Gas Streams", NASA TN D-267, 1960.
7. Cybulski, R. J. and Baldwin, L. V., "Heat Transfer from Cylinders in Transition from Slip Flow to Free-Molecule Flow", NASA Memorandum 4-27-59E, 1959.
8. Stalder, J. R., Goodwin, G., and Creager, M. O., "A Comparison of Theory and Experiment for High-Speed Free-Molecule Flow", NACA Report 1032, 1951.
9. Eimer, M., "Direct Measurements of Laminar Skin Friction at Hypersonic Speeds", GALCIT Hypersonic Wind Tunnel, Memorandum No. 16, 1953.
10. Demetriades, Anthony, "An Experimental Investigation of the Stability of the Hypersonic Laminar Boundary Layer", GALCIT Hypersonic Research Project, Memorandum No. 43, 1958. Also, J. Fluid Mechanics, Vol. 7, No. 3, pp. 385-396, 1960.
11. Morkovin, M. V., "Fluctuations and Hot-Wire Anemometry in Compressible Flows", AGARDograph 24, 1956.
12. Van Der Hegge Zijnen, B. G., "Heat Transfer from Horizontal Cylinders to a Turbulent Air Flow", App. Sci. Res., Vol. 7, Sect. A, pp. 205-223, 1958.
13. Collis, D. C. and Williams, M. J., "Molecular and Compressibility Effects on Forced Convection of Heat from Cylinders", Australian Aero. Res. Lab. Report ARL/A.110, 1958.

14. Tewfik, O. K. and Geidt, W. H., "Local Heat Transfer, Recovery Factor, Pressure Distribution around a Circular Cylinder Normal to a Rarefied Supersonic Air Stream", Proceedings of the 1959 Heat Transfer and Fluid Mechanics Institute.
15. Hayes, W. D. and Probstein, R. F., "Hypersonic Flow Theory", Academic Press, 1959.
16. Hilsenrath, J., Beckett, W. S., et al., "Tables of Thermal Properties of Gases", N. B. S. Circular 564, 1955.
17. "Handbook of Chemistry and Physics", 35th Edition, Chemical Rubber Publishing Co., Cleveland, Ohio, (1953).
18. Kovasznay, L. S. G. and Törmarck, S. I. A., "Heat Loss of Hot-Wires in Supersonic Flow", Bumblebee Report No. 127, Johns Hopkins University, 1950.
19. Spangenberg, W. G., "Heat Loss Characteristics of Hot-Wire Anemometers at Various Densities in Transonic and Supersonic Flow", NACA TN 3381, 1955.
20. McAdams, "Heat Transmission", Third Ed., McGraw-Hill, New York, 1954.
21. Baldwin, L. V., "Slip-Flow Heat Transfer from Cylinders in Subsonic Airstreams", NACA TN 4369, 1958.
22. Christiansen, W. H., "Development and Calibration of a Cold Wire Probe for Use in Shock Tubes", GALCIT Hypersonic Research Project, Memorandum No. 62, July 1, 1961.
23. Cole, J. D. and Roshko, A., "Heat-Transfer from Wires at Reynolds Numbers in the Oseen Range", Proceedings of the 1954 Heat Transfer and Fluid Mechanics Institute.
24. Collis, D. C. and Williams, M. J., "Two-Dimensional Convection from Heated Wires at Low Reynolds Numbers", J. Fluid Mech., Vol. 6, pp. 357-384, 1959.
25. Levy, H. C., "Heat Transfer in Slip Flow at Low Reynolds Number", J. Fluid Mech., Vol. 6, pp. 385-391, 1959.
26. Hurlbut, F. C., "Notes on Surface Interaction and Satellite Drag", RAND Symposium on Aerodynamics of the Upper Atmosphere, June, 1959.
27. Beckwith, I. E., "Similar Solutions for the Compressible Boundary Layer on a Yawed Cylinder with Transpiration Cooling", NASA TR R-42, 1959.

28. Probst, R. F. and Kemp, N. H., "Viscous Aerodynamic Characteristics in Hypersonic Rarefied Gas Flow", J. Aerospace Sci., Vol. 27, No. 3, pp. 174-192, 1960.
29. Willis, D. R., "On the Flow of Gases under Nearly Free Molecular Conditions", Princeton University, Dept. of Aero. Eng., Report No. 442, December, 1958.
30. McClellan, R., "Equilibrium Temperature and Heat Transfer Characteristics of Hot Wires in Supersonic Flow", Ae. E. Thesis, California Institute of Technology, Pasadena, 1955.
31. Winovich, W. and Stine, H. A., "Measurements of the Non-Linear Variation with Temperature of Heat-Transfer Rate from Hot Wires in Transonic and Supersonic Flow", NACA TN 3965, 1957.
32. Van Dyke, M., "Second-Order Boundary-Layer Theory for Blunt Bodies in Hypersonic Flow", ARS Paper No. 1966-61. Presented at the International Hypersonics Conference, Cambridge, Mass., August, 1961.

APPENDIX A

END LOSS CORRECTIONS FOR THE TRANSITIONAL REGIME

In interpreting hot-wire measurements in low density flows, it is imperative that the heat loss to the wire supports be accurately taken into account. For high Reynolds number flow where the convective heat transfer is large and end loss corrections are small, the derivation given by Kovasznay¹⁸ is adequate. However, considerable care must be exercised when these corrections amount to 20 per cent or more of the measured quantity.

Formulation of the Problem

Neglecting radiation, we may write the following heat balance for a small wire element of length dz :

$$\pi d \ell h (T - T_{awm}) = \left(\frac{\pi d^2 \ell}{4} \right) (d/dz) (k_w \frac{dT}{dz}) + i^2 R \quad (A-1)$$

where the left side of the equation represents the convective heat loss, the first term on the right hand side is the net heat added by conduction, and $(i^2 R)$ is the electrical dissipation. Solution of this equation involves the following assumptions:

(a) h , the convective heat transfer coefficient, is a constant and is equal to the value which would be measured by an infinite wire at the same current. This implies that the external flow is uniform along the wire.

(b) The wire thermal conductivity, k_w , is constant.

(c) Wire resistance varies linearly with temperature:

$$\begin{aligned} \frac{R}{R_{awm}} &= \frac{1 + \alpha_r (T - T_r)}{1 + \alpha_r (T_{awm} - T_r)} \equiv 1 + st \\ s &= \frac{\alpha_r T_o}{1 + \alpha_r (T_{awm} - T_r)} \\ t &= (T - T_{awm})/T_o \end{aligned} \quad (A-2)$$

(d) Each cross-section of the wire is at uniform temperature
[implicit in Eq.(A-1)] .

(e) Both wire supports are maintained at a temperature
 $T_s = \eta_s T_o$. * The boundary conditions are thus

$$z = \pm \frac{\ell}{2}, \quad t = t_w = (T_s - T_{awm})/T_o \quad (A-3)$$

With the above boundary conditions, Eq. (A-1) may be integrated to give

$$\begin{aligned} t &= \frac{1}{\nu^2 s} \left[\left(\frac{\ell}{d} \right)^2 \left(\frac{k_o}{k_w} \right) Nu_o (1 + \epsilon s) - \nu^2 \right] \left[1 - \frac{\cosh 2\nu(z/\ell)}{\cosh \nu} \right] \\ &+ t_s \frac{\cosh 2\nu(z/\ell)}{\cosh \nu} \end{aligned} \quad (A-4)$$

where

$$\begin{aligned} \nu^2 &= \left(\frac{\ell}{d} \right)^2 \left(\frac{k_o}{k_w} \right) Nu_o - \frac{i^2 R_{awm} \ell s}{\pi d^2 k_w T_o}, \\ \epsilon &= \eta_s - \eta_m. \end{aligned}$$

The average wire temperature at any given current is

$$\begin{aligned} t &= \int_{-\ell/2}^{\ell/2} t dz = \frac{1}{\nu^2 s} \left[\left(\frac{\ell}{d} \right)^2 \left(\frac{k_o}{k_w} \right) Nu_o (1 + \epsilon s) - \nu^2 \right] \left[1 - \frac{\tanh \nu}{\nu} \right] \\ &+ t_s \frac{\tanh \nu}{\nu} \end{aligned} \quad (A-5)$$

* This restriction is not essential although it simplifies the mathematics considerably. The effect of non-uniform flow near the supports may be partially accounted for by an appropriate choice of η_s .

For an infinitely long wire, $(\ell/d) \rightarrow \infty$, $\bar{t} \rightarrow t_*$, $[(\tanh \nu)/\nu] \rightarrow 0$ and

$$\lim_{(\ell/d) \rightarrow \infty} \bar{t} \equiv t_* = \frac{1}{\nu^2 s} \left[\left(\frac{\ell}{d} \right)^2 \left(\frac{k_o}{k_w} \right) \text{Nu}_o (1 + \epsilon s) - \nu^2 \right] .$$

Eq. (A-5) may now be rewritten in the final form

$$\bar{t} = t_* \left(1 - \frac{\tanh \nu}{\nu} \right) + t_s \frac{\tanh \nu}{\nu} . \quad (\text{A-6})$$

This relation is identical to that derived by Kovasznay¹⁸ if we let the support temperature be equal to the wire recovery temperature ($t_s = 0$) and $\epsilon = 0$. It may easily be seen that the wire temperature \bar{t} will always lie between the temperature t_* of an infinite wire and the support temperature t_s . For large end losses (ν small), the mean wire temperature approaches the temperature of the supports.

Nusselt Number Correction

In order to correct Nu_m to the value Nu_o for an infinite wire, we must find the ratio of these two quantities at a given current. In the present nomenclature, this ratio is

$$\mathcal{F}_N = \frac{\text{Nu}_o}{\text{Nu}_m} = \left(\frac{\bar{t}}{t_* - \epsilon} \right) \frac{(1 + st_*)}{(1 + s\bar{t})} . \quad (\text{A-7})$$

Introducing the quantities

$$\xi^2 = \frac{\left[\left(\frac{\bar{t}}{t_* - \epsilon} \right) \text{Nu}_m \right]_{i=0}}{\left[\left(\frac{\bar{t}}{t_* - \epsilon} \right) \text{Nu}_m \right]}$$

$$\tilde{\nu} \equiv (\nu)_{i=0} = \nu (1 + s\bar{t})^{\frac{1}{2}} \xi$$

and defining

$$\omega = (\tanh \nu / \nu) , \quad \tilde{\omega} = (\tanh \tilde{\nu} / \tilde{\nu})$$

we have

$$\epsilon = - t_s \left(\frac{\tilde{\omega}}{1 - \tilde{\omega}} \right) . \quad (\text{A-8})$$

Equations (A-6) and (A-8) must be solved simultaneously for t_* and in terms of the measured quantities of the experiment.

For low overheats τ , we may perform an expansion in the parameter $(s\bar{t})$. From Eqs. (A-6) and (A-8),

$$\left(\frac{\bar{t}}{t_* - \epsilon} \right) = (1 - \omega) \left[1 + G(\epsilon, \bar{t}, t_s) \right] \quad (\text{A-9})$$

where

$$G = - \left(\frac{t_s}{t_* - \epsilon} \right) \frac{\omega - \tilde{\omega}}{(1 - \omega)(1 - \tilde{\omega})} . \quad (\text{A-10})$$

Using the relations

$$(\tilde{\nu}/\nu) = \xi \left[1 + \frac{1}{2} s\bar{t} - \frac{1}{8} (s\bar{t})^2 + \dots \right]$$

and

$$\tanh(\tilde{\nu} - \nu) = \frac{\tanh \tilde{\nu} - \tanh \nu}{1 - \tanh \tilde{\nu} \tanh \nu}$$

a certain amount of manipulation leads to the equation

$$G = \frac{1}{2} t_s s \xi \frac{\tilde{\omega}}{(1 - \tilde{\omega})(1 - \omega)} \left(\frac{\bar{t}}{t_* - \epsilon} \right) \left[1 - \frac{1}{4} (s\bar{t}) + \dots + - \frac{(-1)}{(t_* - \epsilon)} \right] \times \left[1 - \frac{(1 - \tanh \nu \tanh \tilde{\nu})}{\tilde{\omega}} \left\{ 1 - \frac{\nu^2}{3} \left(\frac{\tilde{\nu}}{\nu} - 1 \right)^2 + \dots \right\} \right] . \quad (\text{A-11})$$

At this point, we are able to make some definite arguments about the magnitudes of the terms appearing in Eq. (A-9). The quantity s will in general be of order 1 and if the end loss is to be small, then $\tilde{\omega}$

$$\frac{\tilde{\omega}}{(1 - \tilde{\omega})(1 - \omega)} \ll 1.$$

Since $|t_s| = |(\eta_s - \eta_m)| \ll 1$, G will then be $O(\eta_m - \eta_s)$ if the bracketed quantities in Eq. (A-11) are $O(1)$. The following approximations are now made:

(a) The quantity $(\xi - 1)/(t_* - \epsilon)$ is small, justified by the experimental fact that Nusselt number changes slowly with overheat.

(b) $(1 - \tanh \tilde{\nu} \tanh \nu) \ll 1$. This is strictly true only for large ν , but making this assumption places an upper bound on G and may be checked a posteriori.

Defining

$$v = -\frac{1}{2} t_s \xi (\tilde{\omega}/\omega) \frac{(1 - \omega)}{(1 - \tilde{\omega})} \quad (\text{A-12})$$

we have the form

$$G = -\frac{v \omega}{(1 - \omega)^2} \left(\frac{\bar{t}}{t_* - \epsilon} \right) \left[1 + \dots + O \left\{ (s \bar{t}), \frac{(\xi - 1)}{(t_* - \epsilon)}, (1 - \tanh \nu \tanh \tilde{\nu}) \right\} \right] \quad (\text{A-13})$$

Substituting Eq. (A-13) into Eq. (A-9) and noting that $v \ll 1$, we obtain the final relations

$$\psi_N = \frac{Nu_o}{Nu_m} = \left(\frac{\bar{t}}{t_* - \epsilon} \right) \frac{(1 + s t_*)}{(1 + s \bar{t})} \quad (\text{A-14})$$

$$\left(\frac{\bar{t}}{t_* - \epsilon} \right) = (1 - \omega) \left[1 - \frac{v \omega}{(1 - \omega)^2} \left\{ 1 + \dots + O \left\langle (s \bar{t}), \frac{(\xi - 1)}{(t_* - \epsilon)}, (1 - \tanh \nu \tanh \tilde{\nu}), v^2 \right\rangle \right\} \right] \quad (\text{A-15})$$

$$v = -\frac{1}{2} t_s \xi (\tilde{\omega}/\omega) \frac{(1 - \omega)}{(1 - \tilde{\omega})} \quad (\text{A-16})$$

$$\nu = \left(\frac{\bar{t}}{t_* - \epsilon} \right)^{\frac{1}{2}} \xi \quad (\text{A-17})$$

$$\zeta = (\ell/d) \left[(k_o/k_w) Nu_m \right]^{\frac{1}{2}} \left[\frac{(1 + \epsilon s)}{(1 + s \bar{t})} \right]^{\frac{1}{2}} \quad (A-18)$$

$$\xi^2 = \left[\left(\frac{\bar{t}}{t_* - \epsilon} \right) Nu_m \right]_{i=0} \left[\left(\frac{\bar{t}}{t_* - \epsilon} \right) Nu_m \right]^{-1} \quad (A-19)$$

For the special case of zero overheat, $\bar{t} = 0$, $t_* = \epsilon$, $\nu = \tilde{\nu}$,

$\xi = 1$, and Eqs. (A-6) and (A-8) may be combined to give an explicit form for the Nusselt number correction factor:

$$(\Psi_N)_{i=0} = (1 - \omega) \left[1 - \frac{1}{2} t_s s \left(\frac{\omega}{1 - \omega} \right) - \frac{1}{2} (t_s s)^2 \left(\frac{\omega}{1 - \omega} \right)^2 \right] \quad (A-20)$$

Recovery Factor Correction

From Eq.(A-8), we may easily find the recovery factor corrections to be

$$\Psi_R = \frac{n_*}{n_m} = \left[\frac{1 - (n_s/n_m)}{(1 - \tilde{\omega})} \right] \quad (A-21)$$

$$\bar{\Psi}_R = \frac{\bar{n}_*}{n_m} = 1 + \frac{\tilde{\omega}}{(1 - \tilde{\omega})} \left[1 - \frac{n_c - n_s}{n_m - n_c} \right] \quad (A-22)$$

Computational Procedure

At this juncture, it seems advantageous to illustrate the computational advantages of Eq. (A-15). Neglecting higher order terms, if v and ν are taken to be parameters we have the relations

$$\left(\frac{\bar{t}}{t_* - \epsilon} \right) = f(\nu, v)$$

$$\nu = f \left[\left(\frac{\bar{t}}{t_* - \epsilon} \right), \zeta \right]$$

and hence

$$\left(\frac{\bar{t}}{t_* - \epsilon} \right) = f(\xi, v)$$

$$v = f(\xi, v) .$$

In Figures 13 and 14, $[\bar{t}/(t_* - \epsilon)]$ and $[\omega/(1-\omega)]$ are shown as functions of $(1/\xi)$, with v as a parameter. The quantity S used by Kovaszny is related to ξ by

$$S = \lim_{\epsilon \rightarrow 0} (1/\xi) . \quad (\text{A-23})$$

The analysis of that reference further restricts the solution to cases where $\xi = 1$ and $t_s = 0$.

It may be readily seen from Figure 13 that the parameter v becomes important only in circumstances where the end loss correction is sizeable. To assess the relative magnitude of v and its effect on the solution we take a hypothetical case where the end loss may be expected to be large. Let

$$(k_o/k_w)^{\frac{1}{2}} = .03125, \quad Nu_m = 0.1600, \quad \bar{t} = 0, \quad \xi = 1$$

$$t_s = -0.120, \quad s = \frac{1}{2}, \quad (\mathcal{L}/d) = 250$$

$$\eta_c = .950, \quad \eta_m = 1.020, \quad \eta_f - \eta_c = 0.210 .$$

To start the calculation, assume $\epsilon = 0$. Then from Eq. (A-18)

$$\xi^{(0)} = .03125 \times 0.4 \times 250 = 3.125$$

$$1/\xi^{(0)} = .3200 .$$

From Eq. (A-16), we calculate

$$v = -\frac{1}{2}(-0.120) \cdot \frac{1}{2} = .030$$

and from Figures 13 and 14 we obtain

$$(\bar{t}/t_* - \epsilon)^{(0)} = 0.571, \quad \left[\frac{\omega}{(1-\omega)} \right]^{(0)} = 0.710.$$

Using Eq. (A-15) with $\bar{t} = 0$ and $t_* \equiv \epsilon = 0$,

$$\bar{\Psi}_N^{(0)} = 0.571.$$

The first approximation to the correction factor for $\bar{\eta}_*$ is computed from Eq. (A-22):

$$\bar{\Psi}_R^{(0)} = (\bar{\eta}_*/\bar{\eta}_m)^{(0)} = 1 + 0.710 \left[1 + \frac{0.05}{0.07} \right] = 2.217$$

and

$$\begin{aligned} \epsilon^{(0)} &= (n_f - n_c) \bar{\eta}_m \left(\frac{\bar{\eta}_*}{\bar{\eta}_m} - 1 \right) \\ &= 0.210 \times 0.333 \times 1.217 \\ &= .0852 \end{aligned}$$

The calculation may now be repeated and a second approximation obtained using $\epsilon^{(0)}$. The following results are obtained:

Quantity	Assumed Value	() ⁽⁰⁾	() ⁽¹⁾	() ⁽²⁾
ϵ	0	0.0852	0.0817	0.0817
$\bar{\Psi}_R$	-	2.217	2.167	2.167
$\bar{\Psi}_N$	-	0.571	0.608	0.608

This hypothetical example illustrates several general properties of the solution. Even for large corrections, the iteration scheme rapidly converges to the true value, regardless of the initial choice of ϵ . Further, the magnitudes of the neglected terms in Eq. (A-15) may be evaluated and suitable correction applied before the final iteration.

For finite overheats, ξ will also enter the computation; since ξ appears only as a multiplier of v and is always close to one, its contribution to the computation should be negligible.

Summary

A rapidly convergent procedure for obtaining end loss corrections appropriate to transitional flow is given. Eq. (A-22) indicates that the support temperature may contribute significantly to the correction of the normalized recovery ratio, and unless the end losses are small, it must be accurately known. The support temperature enters the Nusselt number correction only through the parameter v , and unless the parameter ξ is less than 5, it has a negligible effect on the corrected value Nu_0 .

APPENDIX B

MEASUREMENT OF THE WIRE SUPPORT TEMPERATURE

The analysis given in Appendix A shows clearly that the temperature of the hot-wire supports is an important parameter in the interpretation of recovery temperature data. This is particularly true when the normalized parameter $\overline{\eta}_*$ is used, since an error in the determination of the absolute wire temperature is magnified by a factor of five or more in the computation of $\overline{\eta}_*$. For this reason, a special test was conducted to determine the quantity η_s explicitly.

Two .001" diameter wires, one Pt - 10 per cent Rh and one Constantan, were soft-soldered to the tip of one of the hot-wire support needles to form a thermocouple junction. The complete assembly was then placed in the calibrating oven and a curve of e. m. f. vs. junction temperature obtained. The thermocouple wires were terminated in a constant-temperature junction box for both the oven and tunnel tests, thus eliminating spurious e. m. f. sources caused by thermocouple wire-lead wire temperature variation.

The hot-wire support and thermocouple combination was placed in the tunnel to reproduce, as closely as possible, the actual flow conditions encountered in the hot-wire measurements. Since the needle supports tapered from .02" diameter at several calibers to about .01" at the tip, the .001" thermocouple wire was small compared to body dimensions and should have had a small effect on the surrounding flow field. No correction was made for heat loss by conduction along the thermocouple wire.

Measurements of the support temperature were made over the complete range of tunnel conditions for several positions of the thermocouple near the needle stagnation point. These data are shown in Figure 15. The needle tip was roughly ogival in shape (as shown in the insert) and the angle θ used to define the thermocouple location refers to the angle between the surface normal and the free-stream direction at that point. These data indicate that the support temperature was a constant and equal to $0.903 T_o$ over the complete operating range.

This result can be corroborated by a simple dimensional argument. The rate at which heat is supplied to the probe by convection is proportional to $\left[\frac{k_a Nu_o (\Delta T_g)}{d} \right]$, where ΔT_g is the local difference between the actual support temperature and the adiabatic temperature. From point to point within the solid, the heat transfer rate is proportional to $\left[\frac{k_s (\Delta T_s)}{x} \right]$ where ΔT_s is the temperature difference between two points a distance x apart and k_s is the thermal conductivity of the support. The ratio of the two temperature differences is thus of order

$$(\Delta T_s / \Delta T_g) \sim (k_a / k_s) (x/d) Nu_o .$$

The ratio (k_a / k_s) for air and a steel needle is of order 10^{-4} ; hence $\Delta T_s \ll \Delta T_g$, and the needle is very close to constant temperature throughout.

Let us carry the argument one step further. The free-stream Reynolds number based on support diameter is of the order of 10^3 and

a laminar boundary layer will exist along the length of the support. If negligible heat is lost from the hot-wire support itself, then the net integrated heat transfer must be zero. This means that any heat transferred to the support near the stagnation point will rapidly be conducted away and returned to the flow somewhere downstream. By considering the expansion process around a blunt body in hypersonic flow and the size of the stagnation point surface relative to the downstream exposed surface, it is easily seen that the support temperature should be very close to the adiabatic temperature of a laminar boundary layer with local external Mach number M_n (see the insert of Figure 15). Expressed in mathematical terms,

$$(T_s/T_o) \approx \frac{1 + \sqrt{\text{Pr}} \left(\frac{\gamma-1}{2} \right) M_n^2}{1 + \left(\frac{\gamma-1}{2} \right) M_n^2},$$

where M_n is of order 2.5 to 3 for a blunt ogival body in hypersonic flow. This result agrees with the experimental value to high precision.

APPENDIX C

THE EFFECT OF OVERHEAT ON NUSSELT NUMBER

During the course of this investigation, a few preliminary measurements were made to determine the effect of overheat on the measured Nusselt number. From the results of McClellan³⁰ and Spangenberg¹⁹, it was not expected that at low overheats and Mach numbers outside the transonic range any significant effects would be found. However, in the region where slip effects become appreciable, it is not evident a priori that a variation of surface temperature may be neglected. We shall begin by discussing the data obtained, and conclude with a qualitative description of the results of this and several other investigations.

The present data for $\tau = \frac{T_w - T_{aw}}{T_{aw}} > 0$ were obtained by a procedure identical to that described in Section II. For finite overheat, the variation of wire resistance with heating current must be considered, and Equation (2) is the appropriate computational relation. Four tests were carried out for Reynolds numbers Re_o between 0.5 and 2.0. As can be seen from Figures 8, 9, and 10, the effects (if any) of rarefaction should be very noticeable in this region.

The data of all four tests fell within the shaded region shown in Figure 16. Although the reproducibility of these measurements was not sufficient to discern the influence of Re_o on the $[Nu_o(\tau)/Nu_o(\tau=0)]$ relation, a comparison with the results of McClellan show that even in the slip flow regime, the effect cannot be large for Mach numbers above the transonic range. The difference between the $Re_o \sim 4$ data of

McClellan and the present measurements is probably due to the limited amount of information available from both sources (See McClellan's thesis, p. 19.)

Comparison of the data of Spangenberg at subsonic and transonic speeds with the supersonic and hypersonic data is facilitated by the insert shown in Figure 16. This insert (Figure 22a, Reference 19) is typical of the data available in this range. That the relation between Nusselt number and overheat is quite complex may be seen by comparing the effects of τ for various values of (M/Re) . (See for example Figures 22a-*l*, Reference 19.)

One fact which further complicates the question of the effect of overheat on Nu_o is that none of the available experimental evidence in the transonic range^{7, 19, 21, 31} includes the appropriate data for zero overheat. For example, the data of Spangenberg reproduced in Figure 16 is normalized about the value $\tau = 0.214$. As a comparison, Baldwin²¹ often found as much as a 20 per cent change in the heat transfer coefficient between the values $\tau = 0.07$ and $\tau = 0.22$. Another rather surprising comparison between the works of Baldwin²¹, Cybulski⁷, and Spangenberg is the behavior found at overheats approaching one. As illustrated in Figure 16, Spangenberg found that the change in Nu_o was close to linear with a change in overheat over a large range of Mach and Reynolds numbers. On the contrary, References 7 and 21 show a negligible change in Nu_o when τ is increased beyond about 0.35.

In attempting to interpret these results, it is necessary to distinguish between three separate types of phenomena which are in evidence in these various investigations. The first may be broadly classed as thermodynamic, which would include small changes in the

local temperature of the fluid near the body and the subsequent effects on viscosity, density, Prandtl number and the like. These differences for the most part are small (at least for small overheats or changes in stagnation temperature) and may be accounted for at high Reynolds numbers by using any of the several available compressible boundary layer analyses. The second class may be broadly termed induced flow effects, wherein a change in body temperature is sufficient to alter the basic features of the flow field, and through this "interaction" change the measured heat transfer. Thirdly, the effect of surface temperature on molecular processes must also be considered.

From the above delineation, we may immediately imply several important generalizations. First, in the range of high Reynolds numbers, the effects of overheat should be of the thermodynamic type. Second, as the Reynolds number decreases, a given fractional change in the boundary layer thickness caused by fluid property variation would have an increasing effect on the flow field adjacent to the body. From boundary layer theory, $q \sim (d/2)^{-\frac{1}{2}}$ where d is the diameter of the cylinder. If the boundary layer displacement thickness is not negligibly small, then $q \sim \left[(d/2) \left(1 + \frac{2\delta^*}{d} \right) \right]^{-\frac{1}{2}}$, and an increase in the displacement thickness (i. e., an increase in the wire temperature) would tend to decrease the heat transfer rate to the body. This result agrees with the experimental results given in Figure 16. The third conclusion is that this induced flow effect would be most pronounced in the transonic regime, where the flow field is extremely sensitive to the effective body shape. All of these statements are borne out by the present experiments and the data of Spangenberg¹⁹ and Winovich and Stine³¹. In cases where these different

effects are of the same order, it becomes difficult to separate them by less than rigorous analysis.

Several investigations^{2, 3, 6, 7, 8, 22} have been conducted under conditions approaching free molecule flow. Air, nitrogen, helium, and argon have all been used as test gases for these subsonic and supersonic experiments. In all cases, the test body (a hot-wire, unheated wire or butt-welded thermocouple) was maintained at a temperature differing significantly from the equilibrium recovery temperature. Several interesting but as yet unexplained results were obtained for various combinations of overheat (both positive and negative), test medium, and Mach number. The most important requirement at this time is a working model of the actual interaction process between a rapidly moving molecule and a surface of arbitrary roughness and temperature. As indicated earlier, in free molecule flow the body temperature will change the heat transfer rate only through its effect on the accommodation coefficient.

APPENDIX D

MEASUREMENTS AT REYNOLDS NUMBERS
APPROACHING FREE MOLECULE FLOW

At the conclusion of this investigation, an attempt was made to extend the data to lower Reynolds numbers by using .00005" diameter Pt - 10 per cent RH wires. These tests were not quantitatively repeatable because of possible non-uniformity of the wires, repeated breakage and consequent incomplete calibration, and other reasons which are not yet fully understood. However, each individual wire produced a self-consistent set of heat transfer data.

The accuracy of these measurements was considerably less than the accuracy obtained using .0001" diameter wire. Microscopic examination revealed that these small wires possessed a variety of small "kinks"; whether these non-uniformities were caused by installation, tunnel exposure, or the actual manufacturing process was not clear.

Figure 17 shows that the slope of the $Nu_o - Re_o$ curve obtained with each individual wire was equal to unity within the experimental scatter. Although the slopes agreed quite well, the proportionality constant varied by as much as 40 per cent. Data obtained at high Mach numbers in air and nitrogen by Weltmann and Kuhns⁶ and by Wong³ are included in the figure for comparison. In each of these experiments, the slope of the $Nu_o - Re_o$ curve is again nearly unity within the limits of the data. This fact emphasizes several of the remarks made earlier with reference to Figure 9; between several independent investigations there appears to be better agreement in the slope of the $Nu_o - Re_o$ relation than in the absolute magnitude of the correlation.

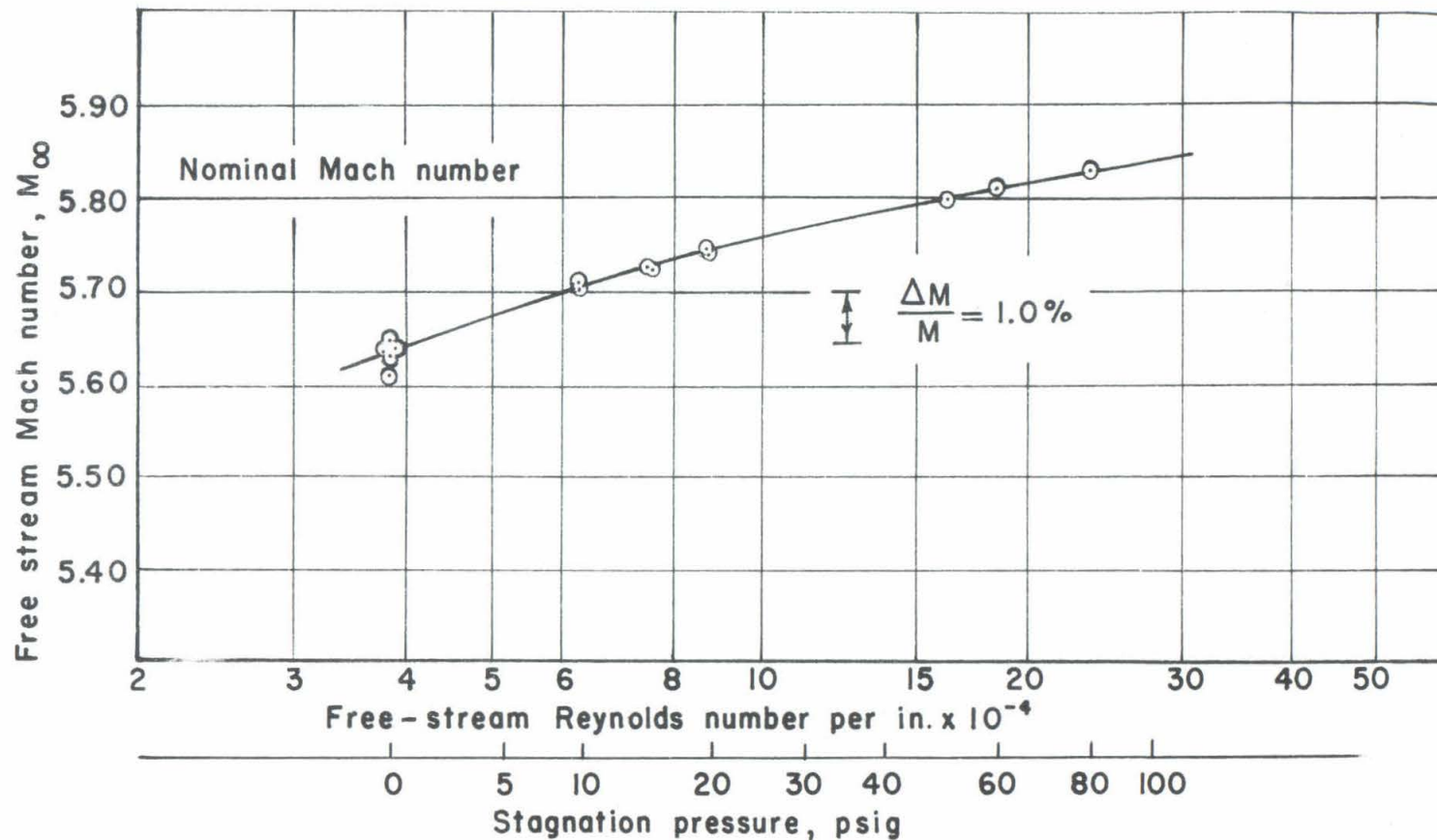


FIG. 1 VARIATION OF FREE STREAM MACH NUMBER WITH TUNNEL PRESSURE

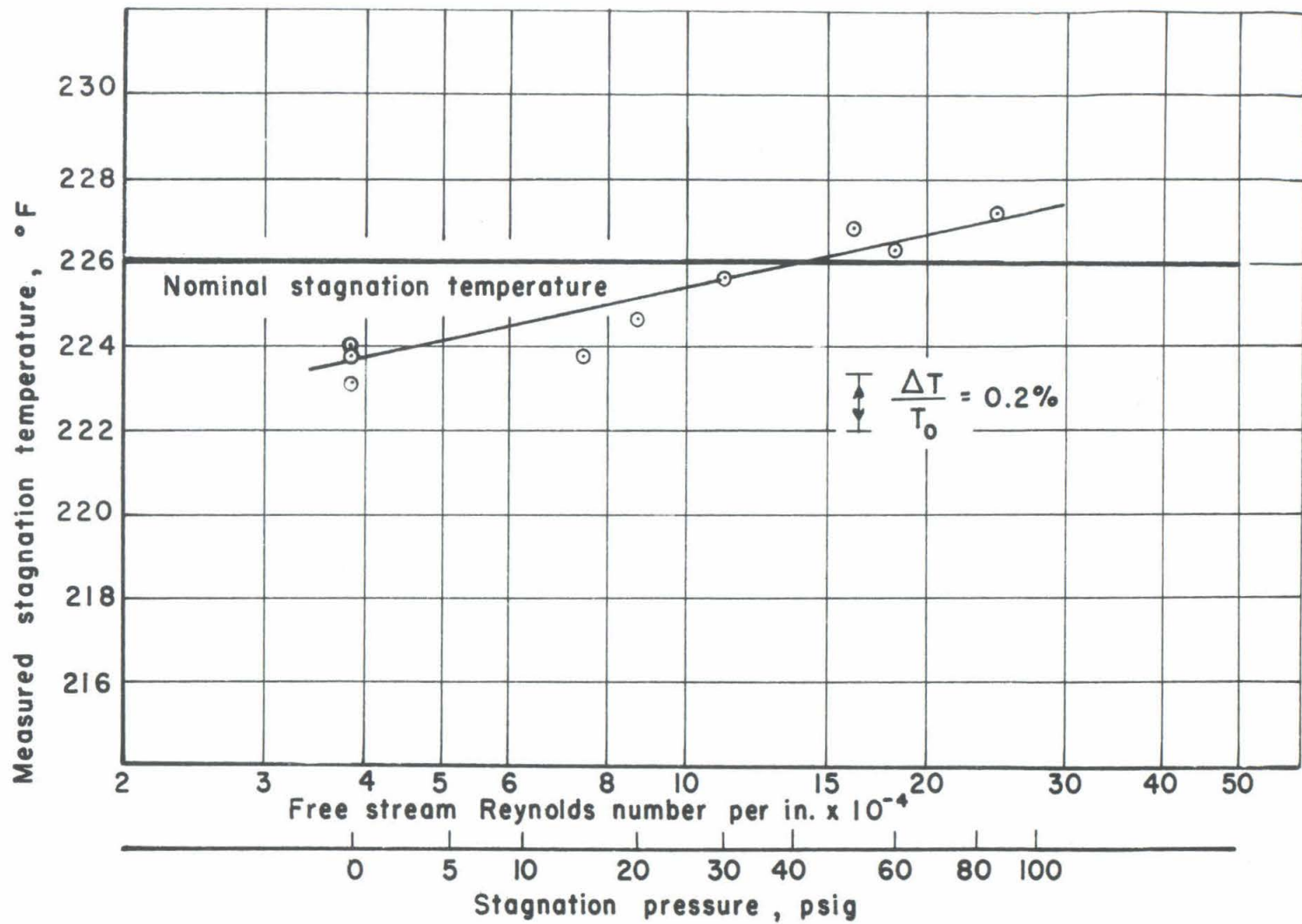
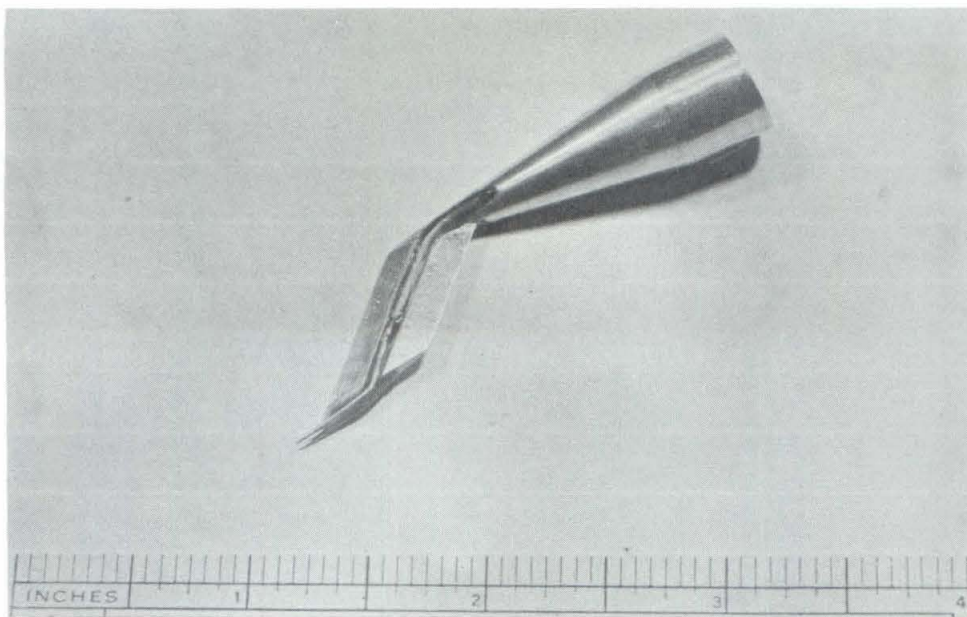
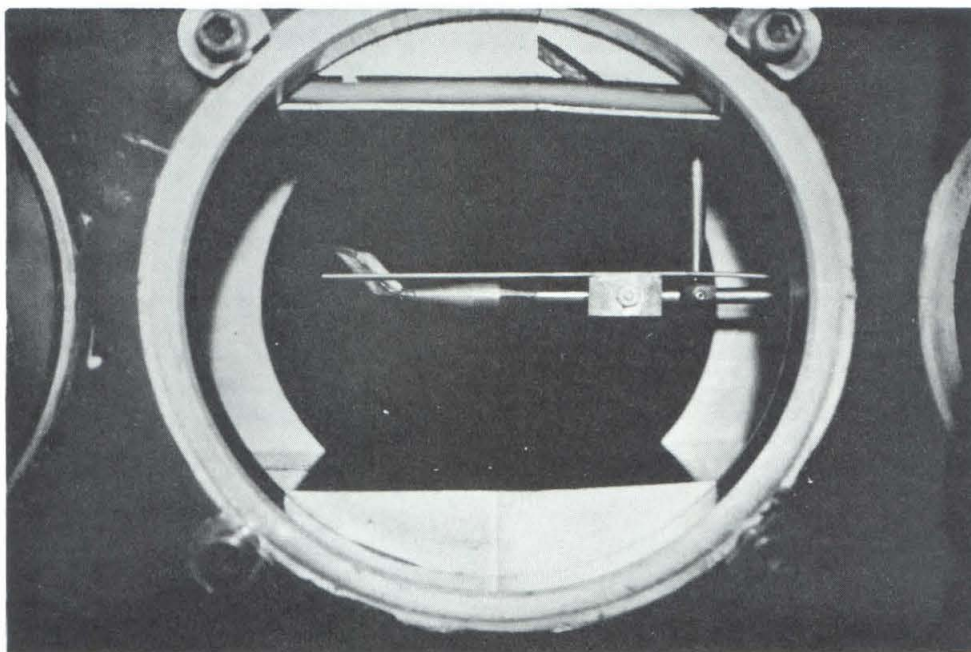


FIG.2 VARIATION OF STAGNATION TEMPERATURE WITH TUNNEL PRESSURE



a) Hot - Wire Probe



b) Hot-Wire Probe and Total Pressure Tube Installed in Tunnel

FIG. 3 HOT-WIRE PROBE AND TUNNEL INSTALLATION

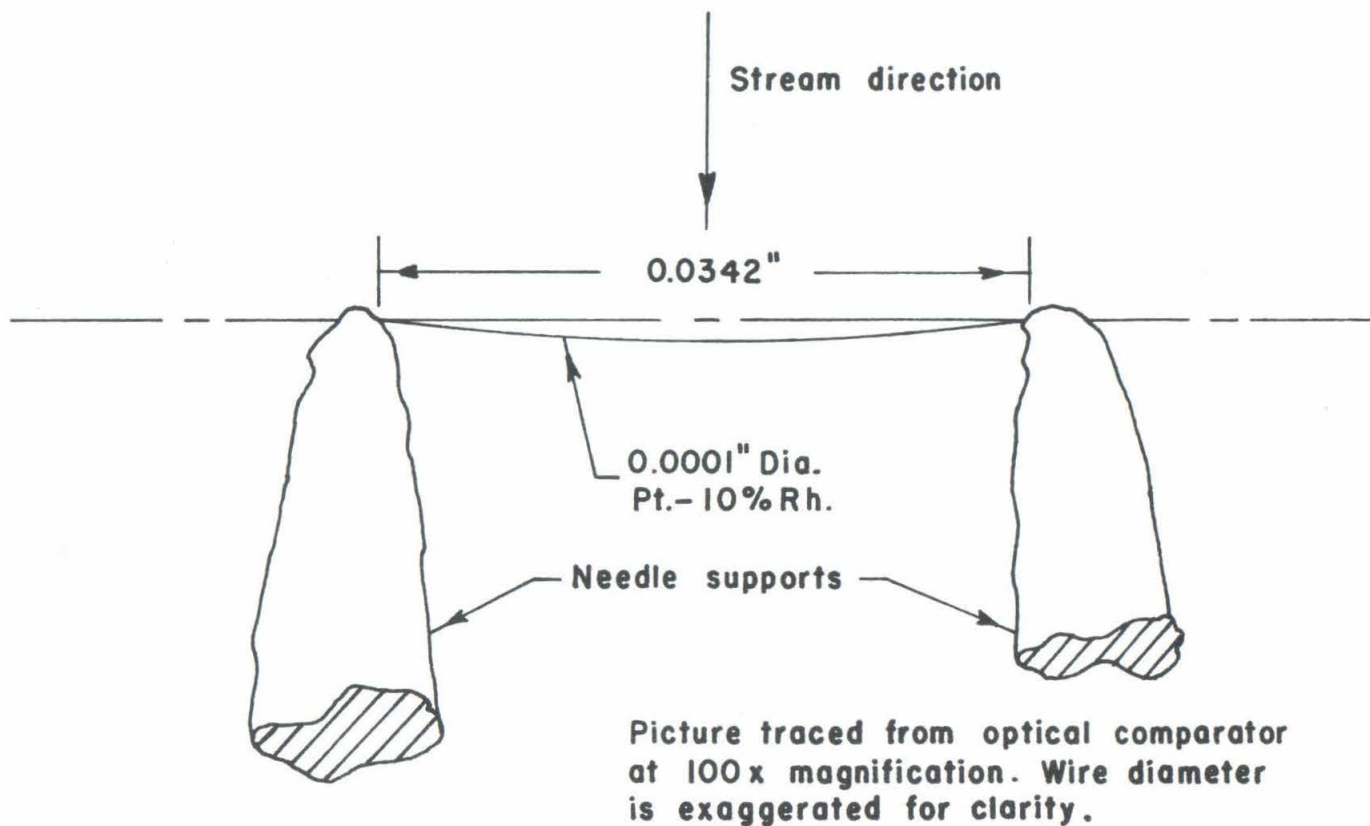


FIG. 4 TYPICAL HOT-WIRE INSTALLATION AFTER TUNNEL EXPOSURE

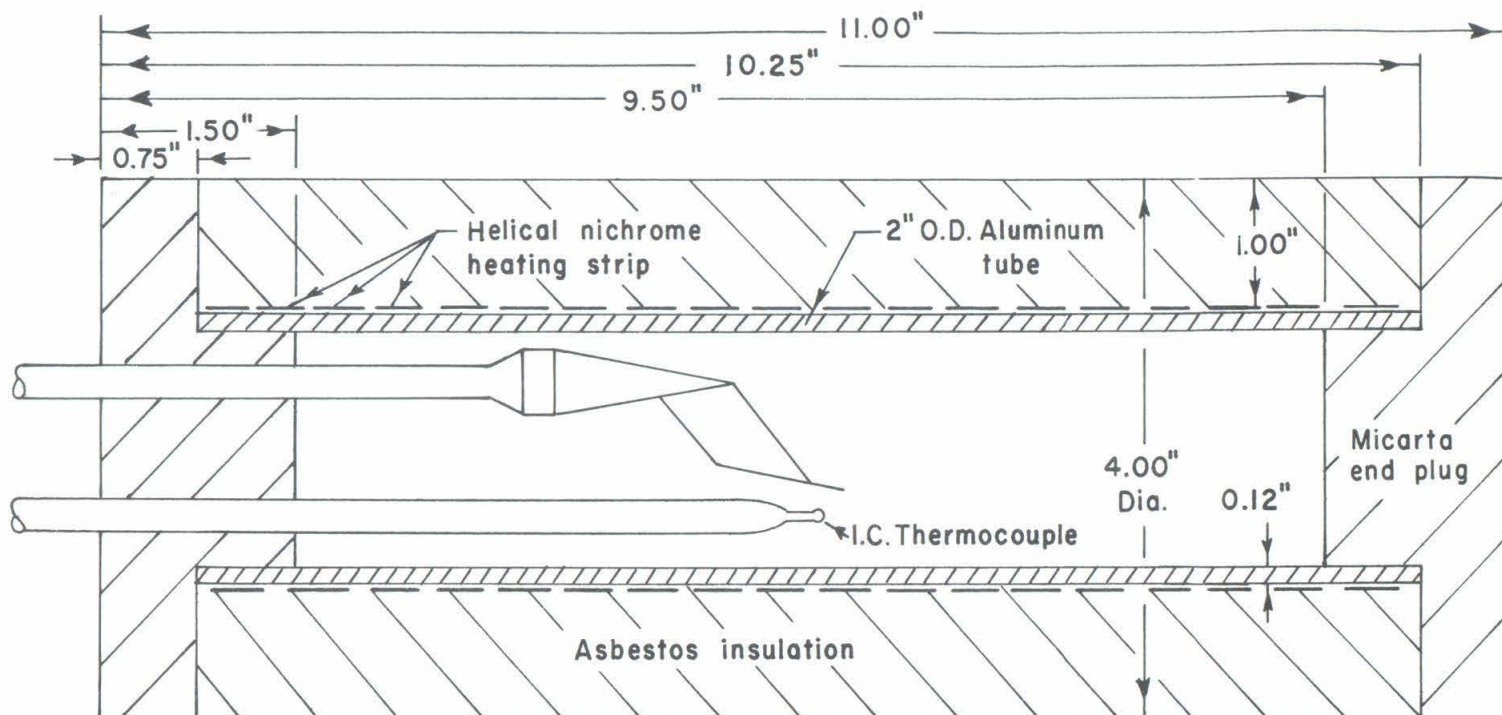
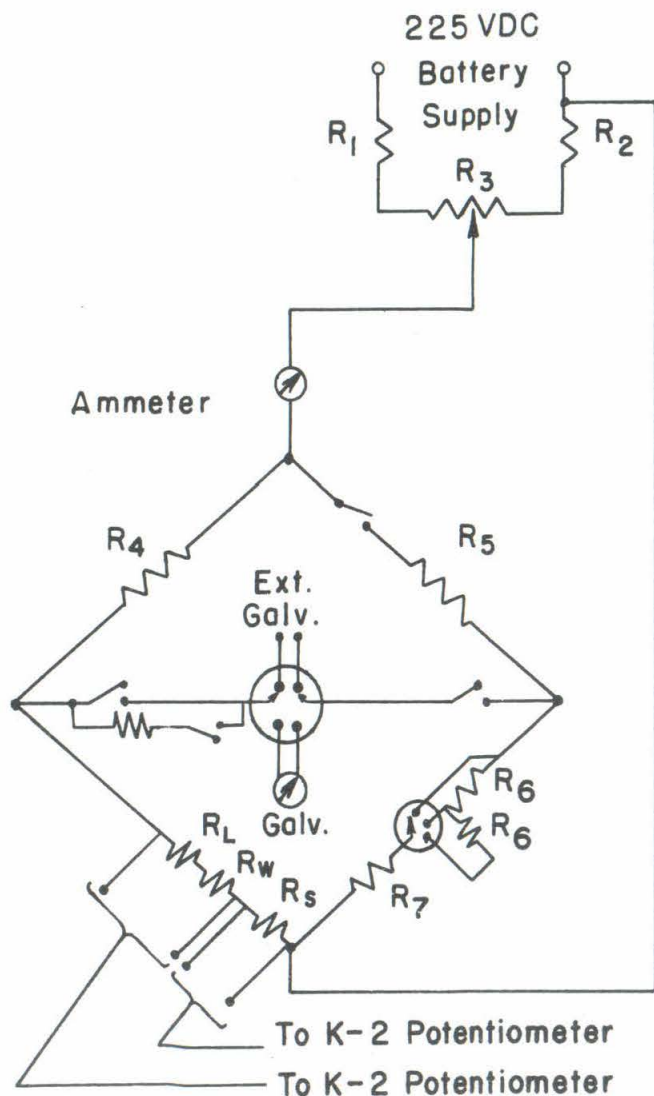


FIG. 5 DIAGRAM OF CALIBRATION OVEN



Resistance Table

	Setting I	II	III	IV
R_1	24 K Ω	18 K Ω	12 K Ω	6 K Ω
R_2	0	6.8 K Ω	16 K Ω	24 K Ω
R_3	0-6 K Ω 15-Turn Helipot ($\pm 0.5\%$ Linearity)			
R_4	7.5 K Ω			
R_5	75 K Ω			
R_6	1 K Ω			
R_7	0-1 K Ω 10-Turn Helipot ($\pm 0.5\%$ Linearity)			
R_W	Hot-Wire ($\sim 40 \Omega$)			
R_L	Line ($\sim 0.6 \Omega$)			
R_S	1.000 $\Omega \pm 0.1\%$ (Standard Resistor)			

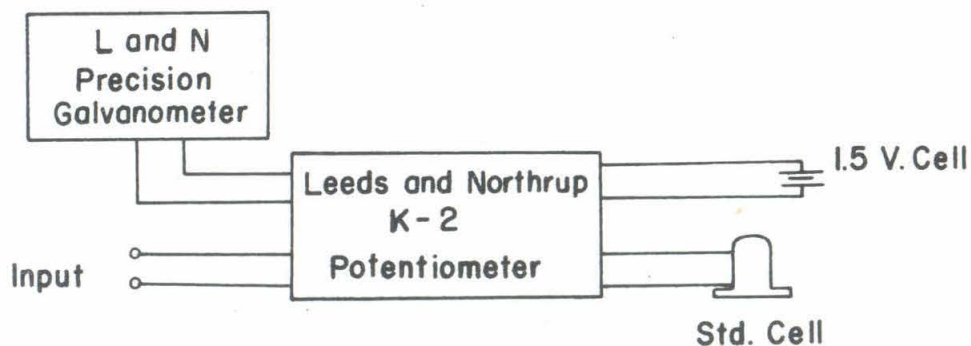


FIG. 6 ELECTRICAL CIRCUIT DIAGRAM

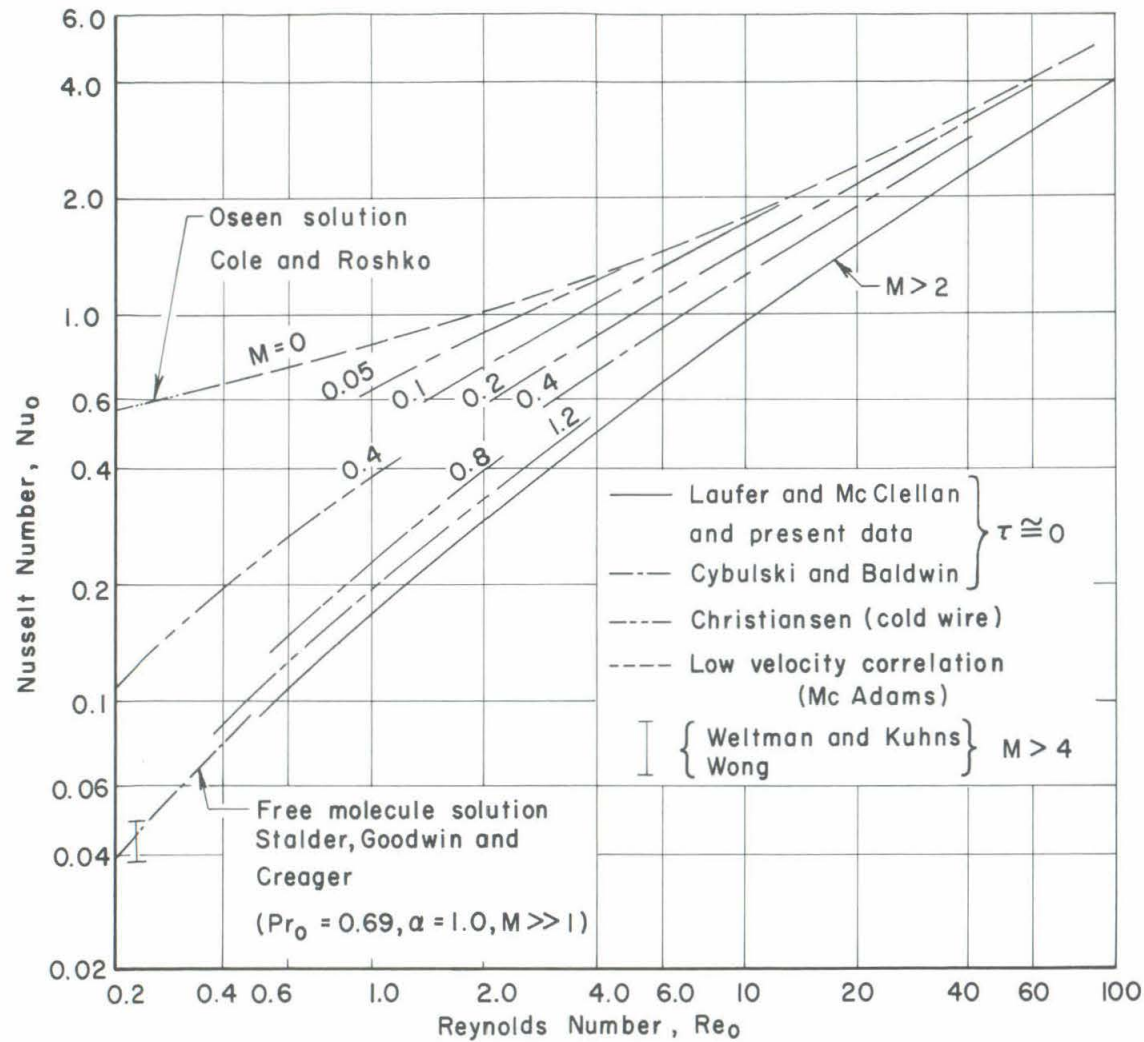


FIG. 7 EMPIRICAL CORRELATION OF HOT-WIRE HEAT TRANSFER AT LOW REYNOLDS NUMBERS

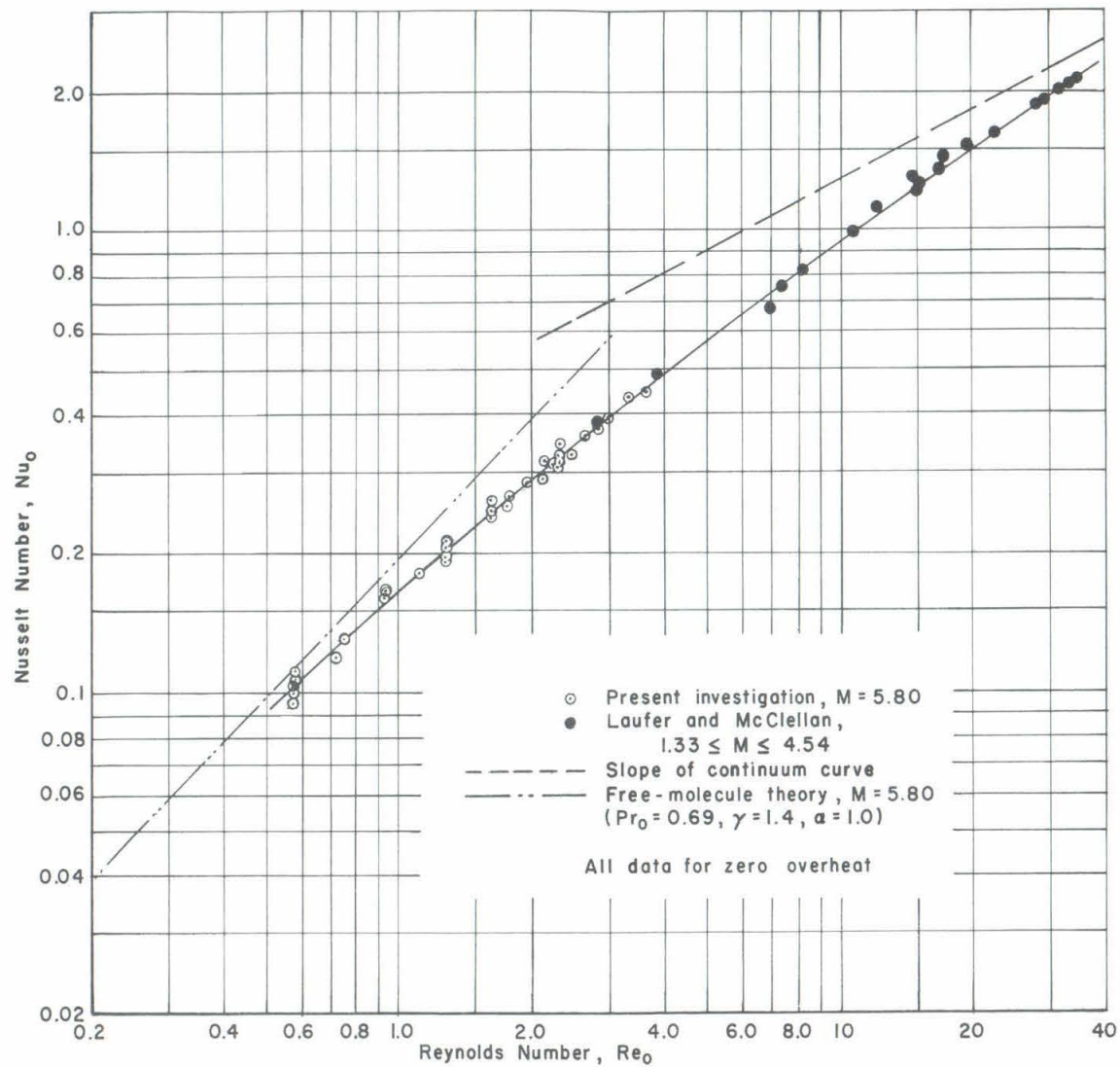


FIG. 8 NUSSELT NUMBER — REYNOLDS NUMBER RELATION FOR SUPERSONIC AND HYPERSONIC FLOW

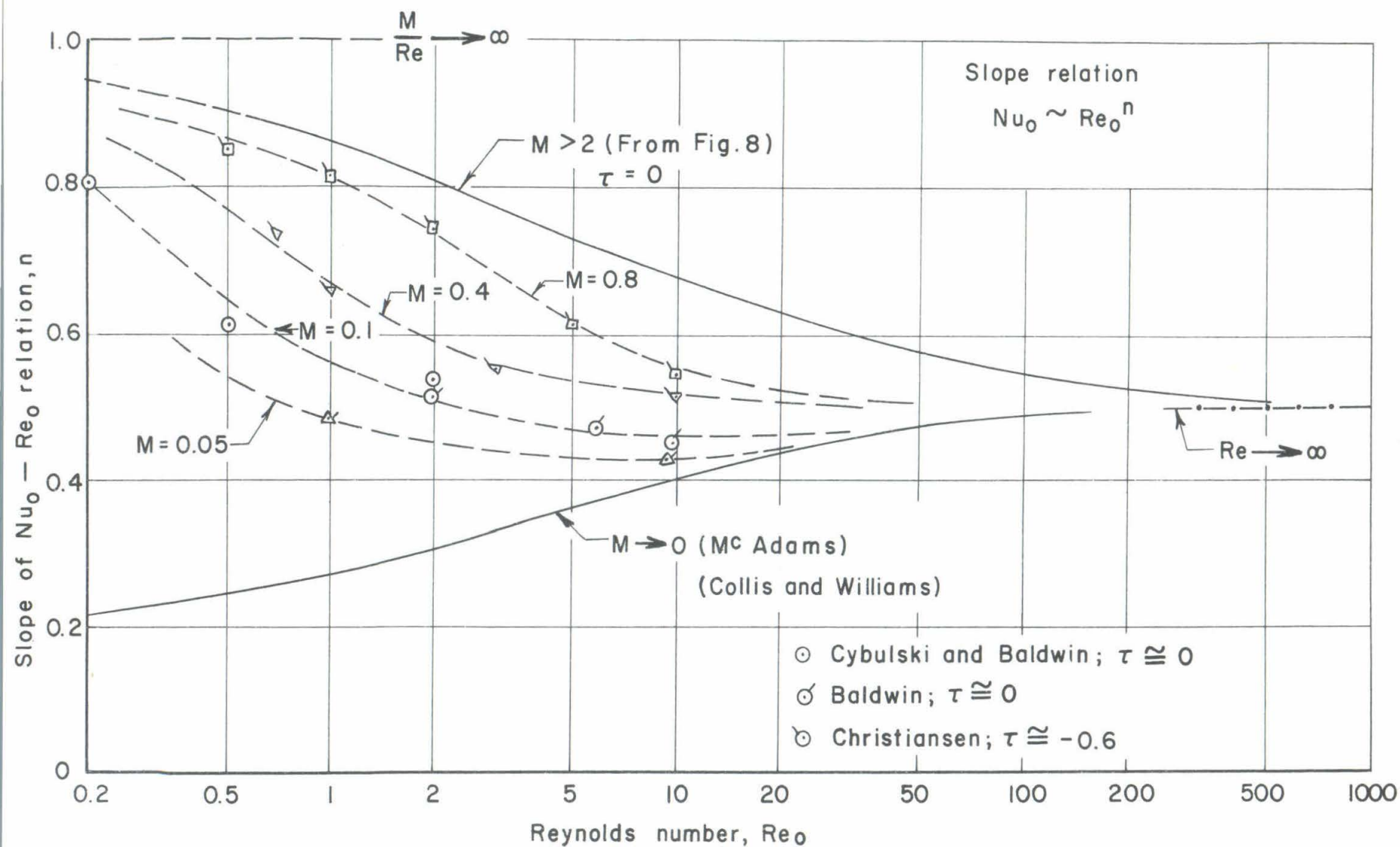


FIG.9 - SLOPE OF NUSSELT NUMBER-REYNOLDS NUMBER RELATION AS A FUNCTION OF REYNOLDS NUMBER

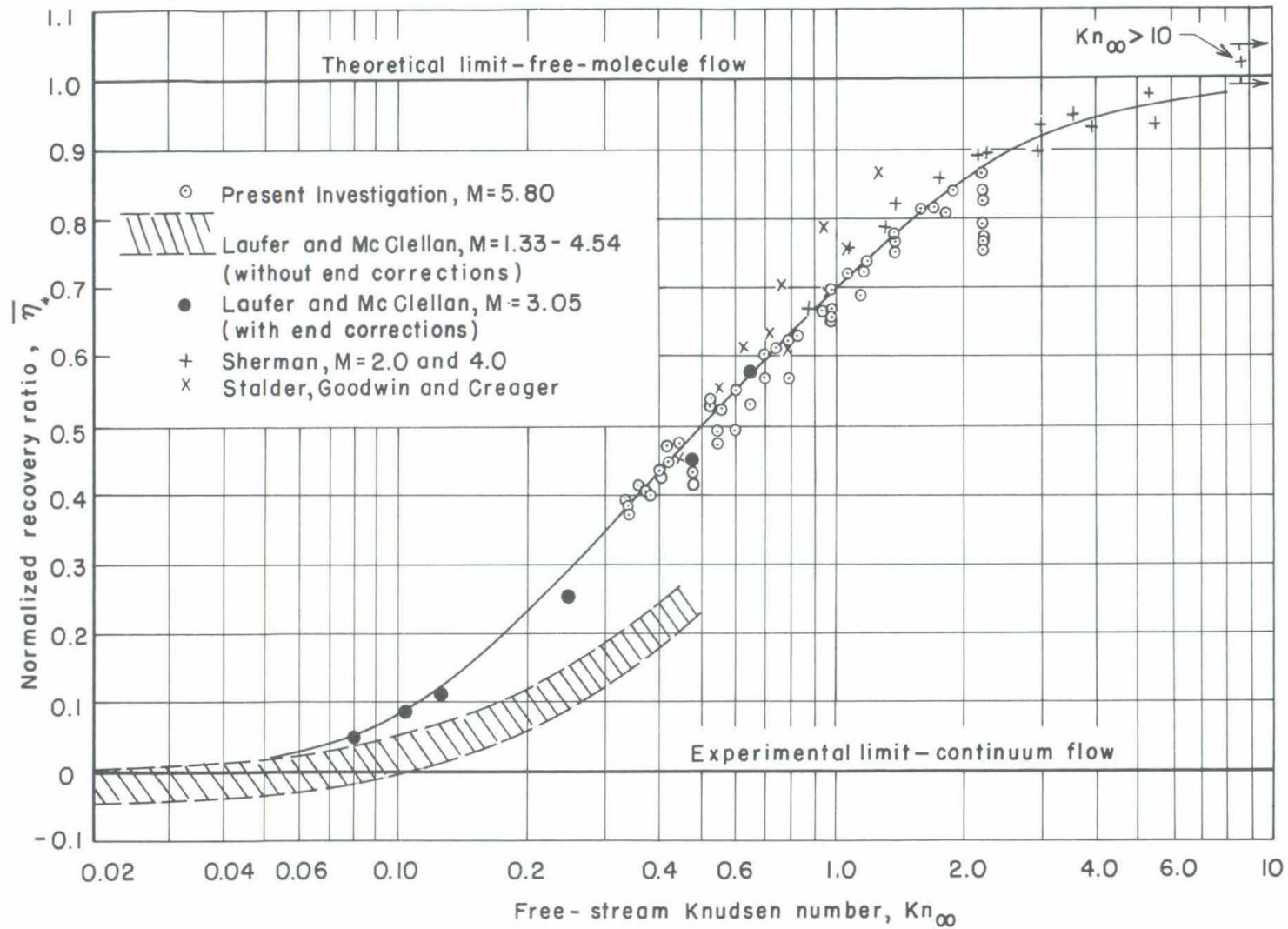


FIG. 10 NORMALIZED VARIATION OF RECOVERY TEMPERATURE WITH KNUDSEN NUMBER

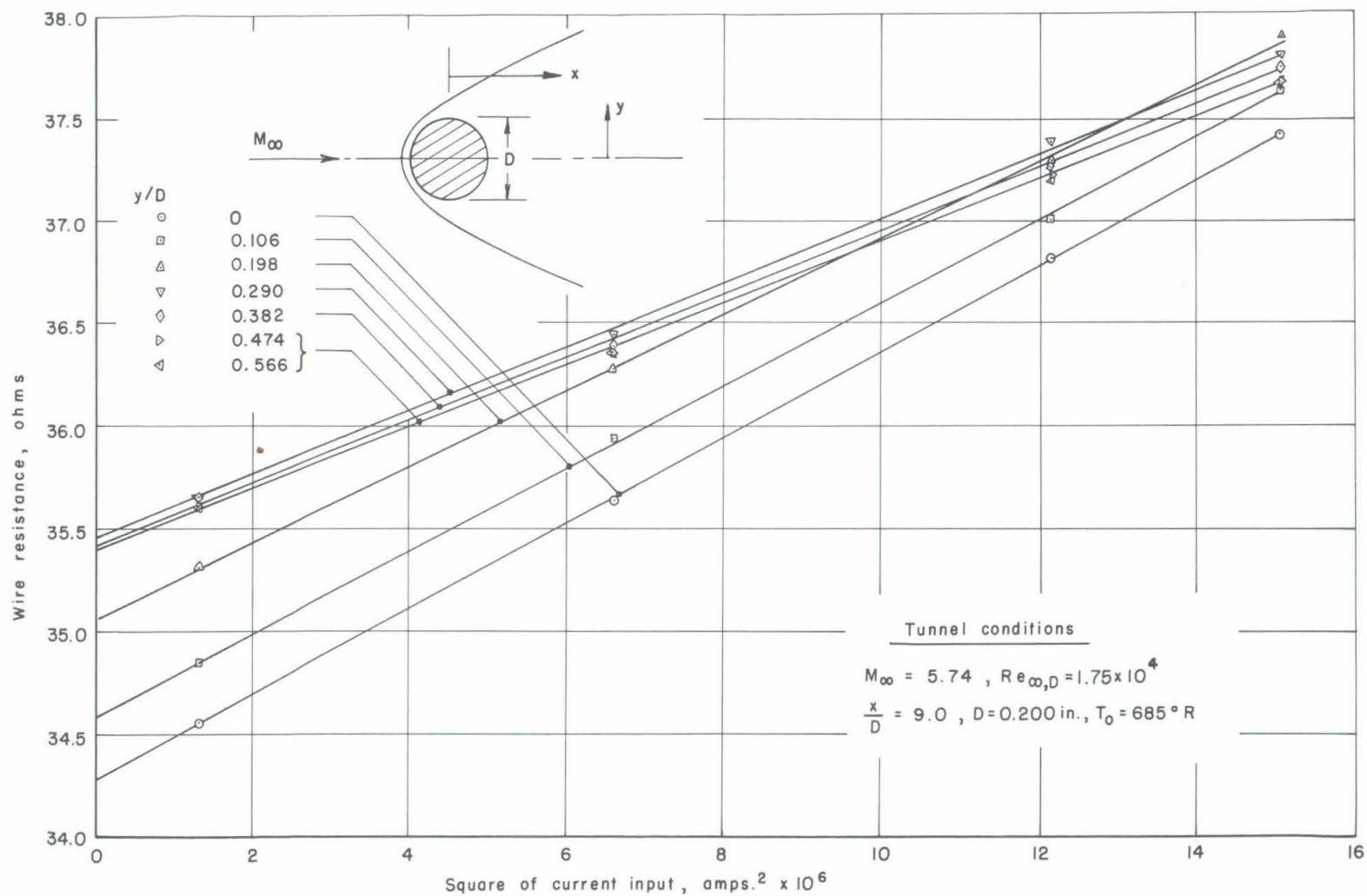
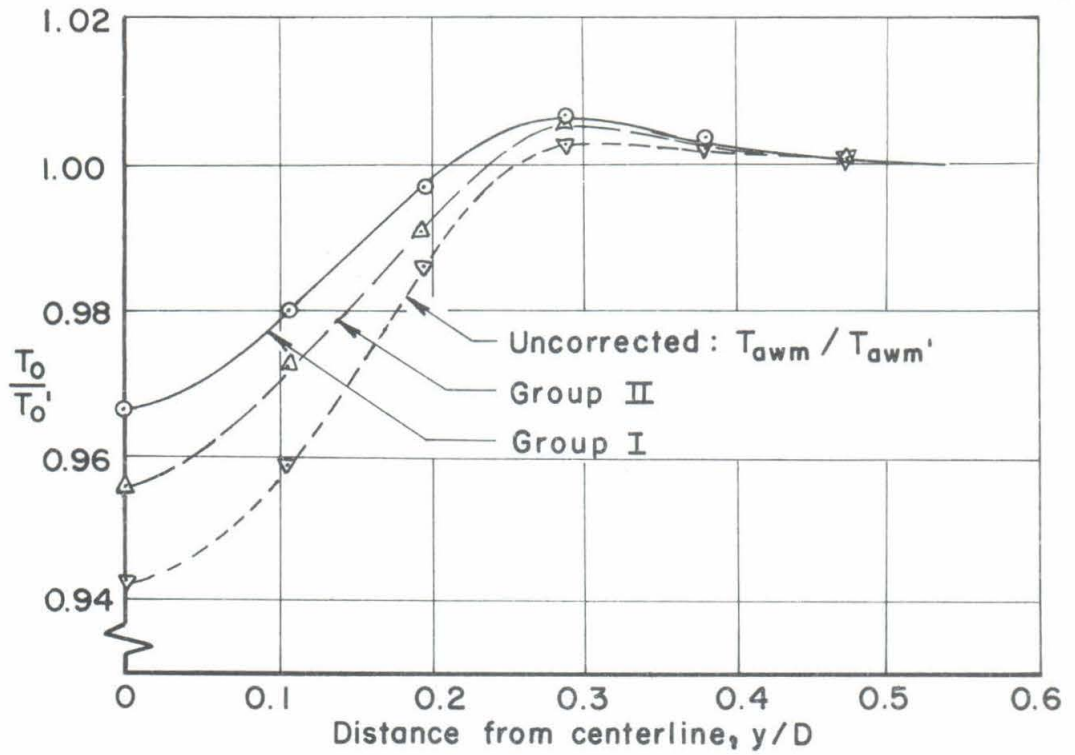
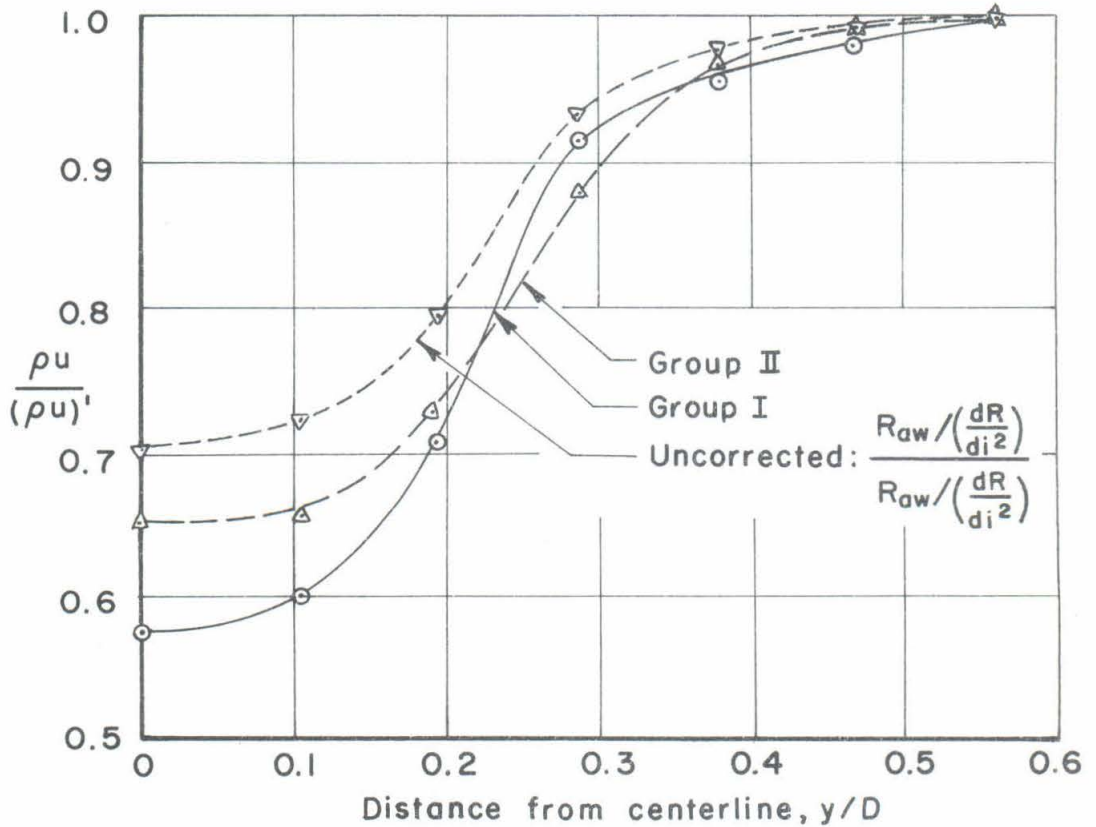


FIG.II - DATA OBTAINED FROM CYLINDER WAKE TRAVERSE

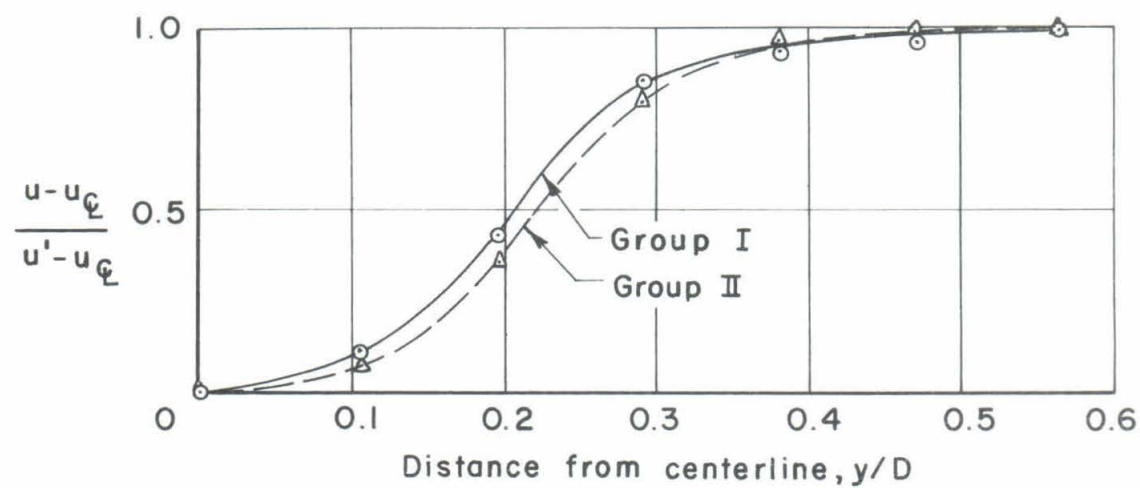


a) Temperature distribution



b) Mass flow distribution

FIG. 12 VARIATION OF FLOW QUANTITIES ACROSS THE CYLINDER WAKE



c) Velocity defect

FIG. 12, Cont'd.

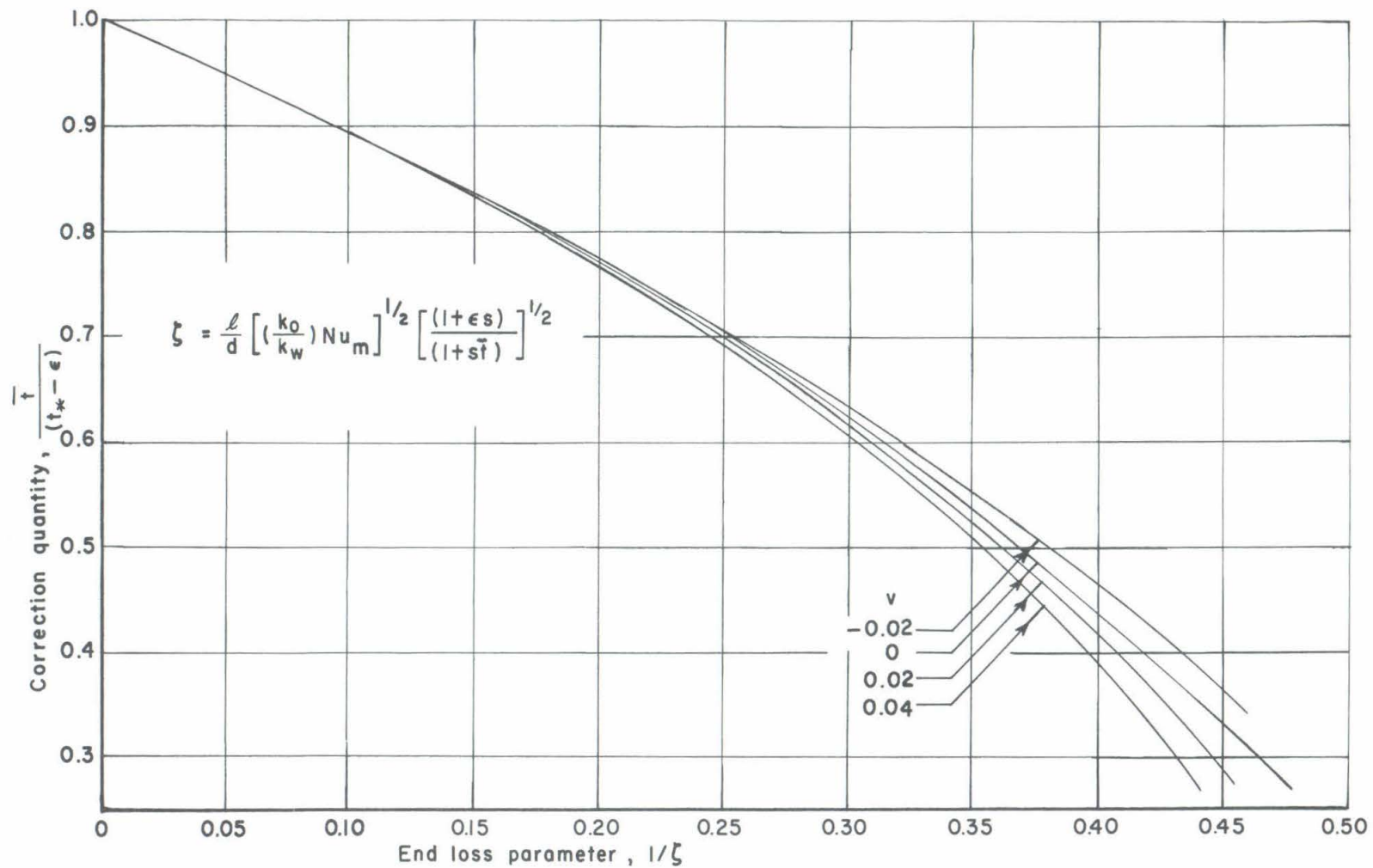


FIG.13 END LOSS RELATIONS FOR NUSSELT NUMBER CORRECTION

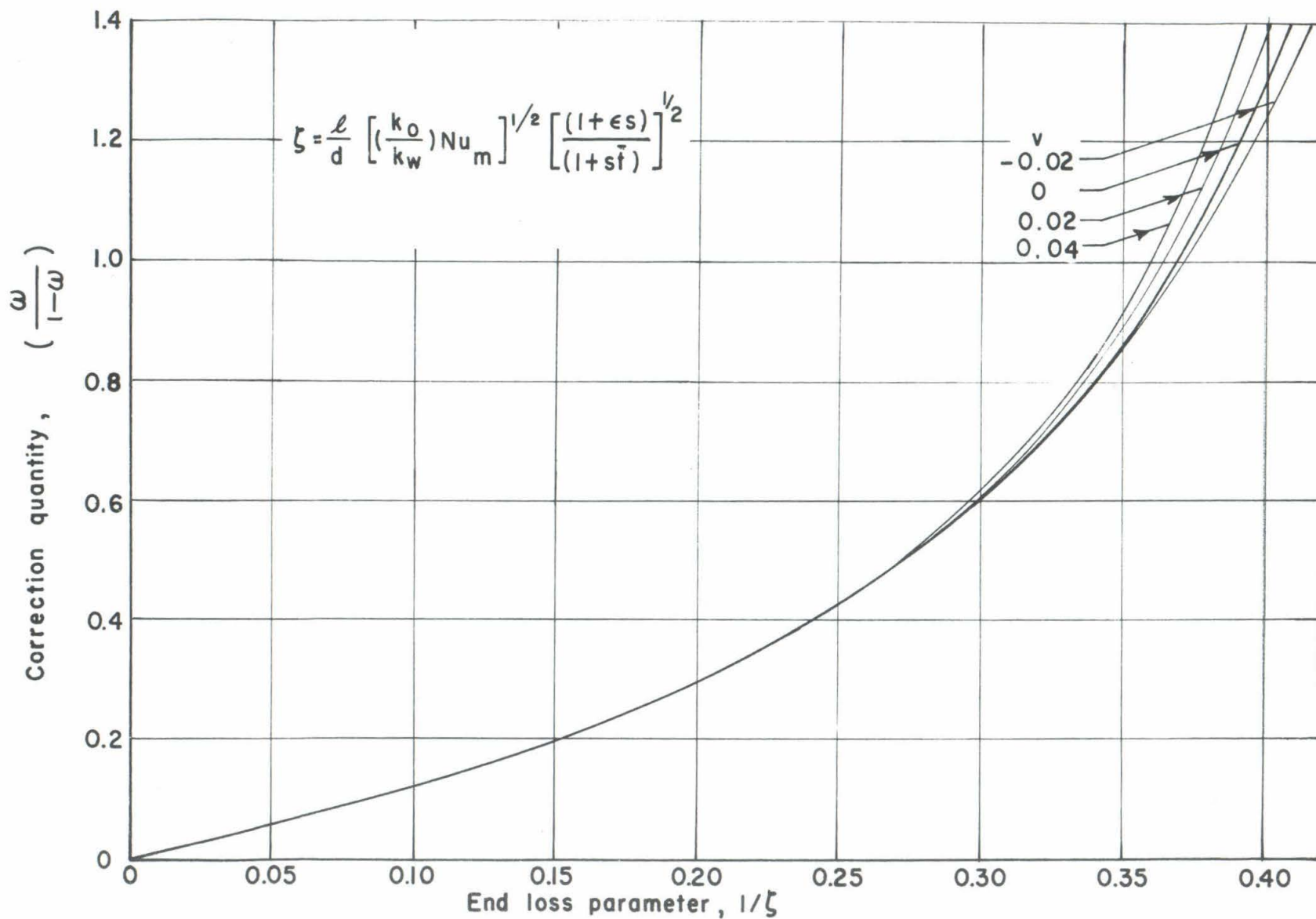


FIG. 14 END LOSS RELATIONS FOR RECOVERY TEMPERATURE CORRECTION

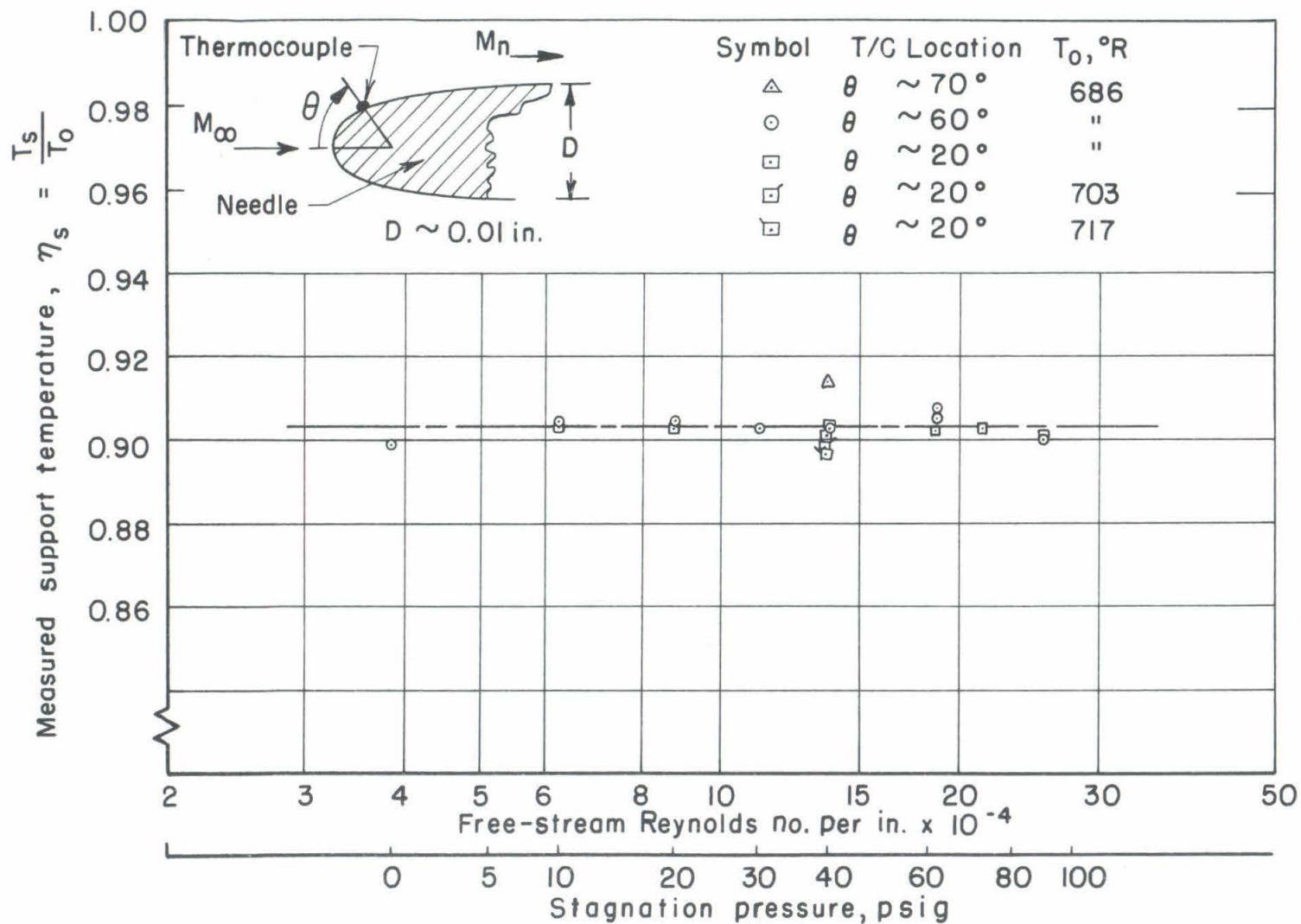


FIG. 15 WIRE SUPPORT TEMPERATURE AS A FUNCTION OF TUNNEL PRESSURE

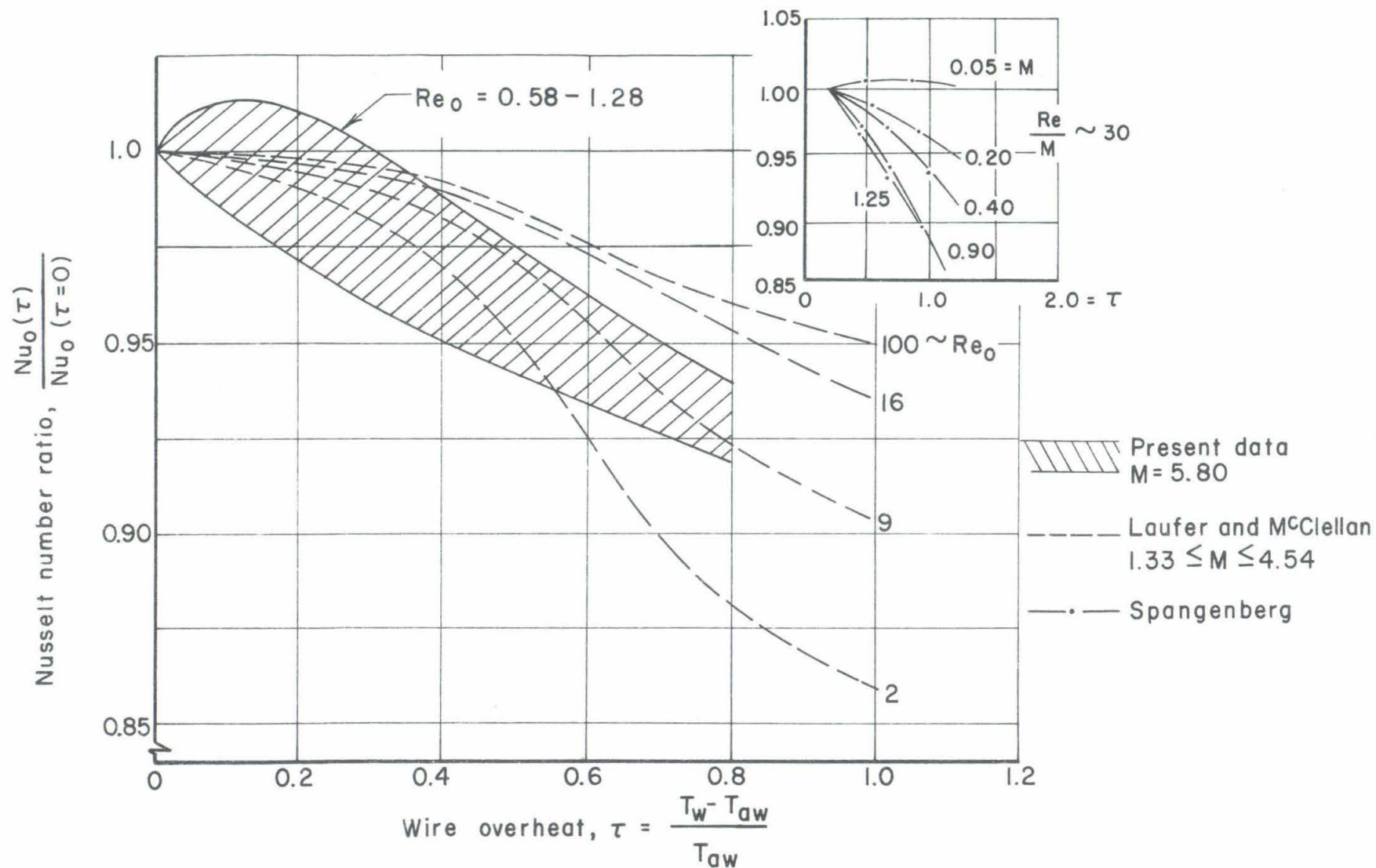


FIG. 16 - VARIATION OF NUSSELT NUMBER WITH OVERHEAT

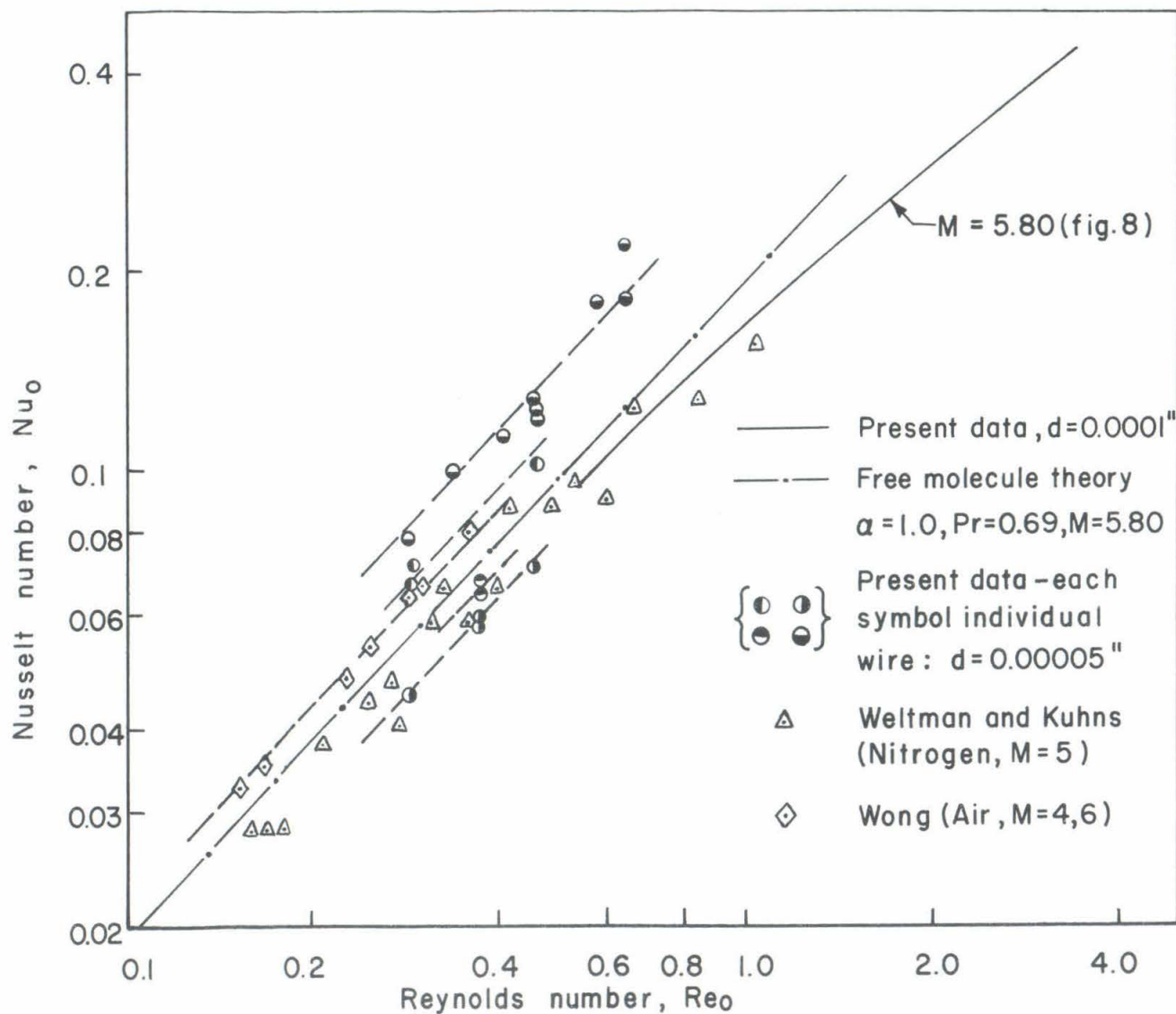


FIG.17 NUSSELT NUMBER-REYNOLDS NUMBER RELATION APPROACHING FREE MOLECULE FLOW

DISTRIBUTION LIST

United States Army

U. S. Army Research Office (Durham)
Box CM, Duke Station
Durham, North Carolina
Attention: Information Processing Office
20 copies

Army Rocket and Guided Missile Agency
U. S. Army Ordnance Missile Command
Redstone Arsenal
Alabama
Attention: Technical Library
Attention: Mr. John Morrow
ORDXR-RMO

Commander
Army Ballistic Missile Agency
Redstone Arsenal
Alabama
Attention: ORDAB-IPL

Los Angeles Ordnance District
55 South Grand Avenue
Pasadena 2, California
Attention: Mr. John D. Flanagan,
Acting Branch Chief,
Research Branch

Chief of Ordnance
Department of the Army
ORDTB - Ballistic Section
The Pentagon
Washington 25, D. C.
Attention: Mr. George Stetson

Office of the Chief of Research and
Development
Department of the Army
Army Research Office
Washington 25, D. C.
Attention: Chief, Research Support Division

Commanding Officer
Diamond Ordnance Fuze Laboratories
Washington 25, D. C.
Attention: ORDTL 012

U. S. Army Ordnance
Ballistic Research Laboratories
Aberdeen Proving Ground
Maryland
Attention: Dr. Joseph Sternberg, Chief
Exterior Ballistics Laboratory
Attention: Dr. Raymond Sedney
Exterior Ballistics Laboratory

Commanding General
White Sands Missile Range
New Mexico
Attention: Technical Library

United States Navy

Director
U. S. Naval Research Laboratory
Washington 25, D. C.

U. S. Naval Ordnance Laboratory
White Oak
Silver Spring, Maryland
Attention: Dr. R. Kenneth Lobb
Aeroballistics Program Chief
Attention: Dr. A. E. Seigel
Chief, Ballistics Department
Attention: Dr. R. E. Wilson
Associate Technical Director
(Aeroballistics)

U. S. Naval Weapons Laboratory
Dahlgren, Virginia
Attention: Technical Library

U. S. Navy Department
David Taylor Model Basin
Applied Mathematics Laboratory
Washington 7, D. C.
Attention: Dr. F. N. Frenkiel

United States Air Force
Air Research and Development Command

Aeronautical Research Laboratories
Air Force Research Division
Air Research and Development Command
United States Air Force
Wright-Patterson Air Force Base
Ohio
Attention: Mr. Fred L. Daum, RRLD
Attention: Dr. Karl Gottfried Guderley, RRLM
Attention: Dr. Roscoe H. Mills, RRLD
Attention: RRL

Wright Air Development Division
Air Research and Development Command
United States Air Force
Wright-Patterson Air Force Base
Ohio
Attention: WADD (WWAD - Library)
Attention: WADD (WWFEA - Reports Unit)
Attention: ASD(ASRMDF, Mr. Philip P. Antonatos)

Air Force Office of Scientific Research
Air Research and Development Command
United States Air Force
Washington 25, D. C.
Attention: Mechanics Division; Milton Rogers, Chief
Attention: SRGL (2 copies)

Directorate of Research Analysis
Air Force Office of Scientific Research
Air Research and Development Command
United States Air Force
Holloman Air Force Base
New Mexico
Attention: SRLS, Dr. Gerhard R. Eber

Air Force Ballistic Missile Division
Air Research and Development Command
United States Air Force
Air Force Unit Post Office
Los Angeles 45, California
Attention: Advanced Systems Division (WDTVV-3); Major E. W. Geniesse, Jr.
Attention: Penetration Division (WDTVV-4); 1/Lt. H. E. Hunter
Attention: AVCO Re-entry Vehicles Division (WDTVV-1); Capt. G. S. Lewis, Jr.

Air Research and Development Command
United States Air Force
Eglin Air Force Base
Florida
Attention: APGC (PGTRI, Technical Library)

Armed Services Technical Information Agency
Air Research and Development Command
United States Air Force
Arlington Hall Station
Arlington 12, Virginia
Attention: ASTIA (TIPCA) -- 10 copies

National Aeronautics and Space Administration

NASA

Headquarters
1520 H Street, Northwest
Washington 25, D. C.
Attention: Dr. H. H. Kurzweg
Assistant Director of Research

NASA

George C. Marshall Space Flight Center
Huntsville, Alabama
Attention: Dr. Ernst D. Geissler, Director, Aeroballistics Division
Attention: M-AERO-A, Mr. Werner K. Dahm
Attention: Aeroballistics Division, M-AERO-E, Mr. T. G. Reed (3 copies)

NASA

Langley Research Center
Langley Field, Virginia
Attention: Librarian
Attention: Mr. Clinton E. Brown, Chief, Theoretical Mechanics Division, Bldg. 1212
Attention: Dr. Adolf Busemann
Attention: Mr. Charles H. McLellan, 11-Inch Hypersonic Tunnel Section

NASA

Ames Research Center
Moffett Field, California
Attention: Library

NASA

Lewis Research Center
21000 Brookpark Road
Cleveland 35, Ohio
Attention: Library, Mr. George Mandel
2 copies

Miscellaneous Government Agencies

United States Atomic Energy Commission
P. O. Box 62
Oak Ridge, Tennessee
Attention: Library

U. S. Department of Commerce
National Bureau of Standards
Washington 25, D. C.
Attention: Dr. G. B. Schubauer
Chief, Fluid Mechanics Section

Universities and Non-Profit Organizations

Brown University
Division of Applied Mathematics
Providence 12, Rhode Island
Attention: Professor R. E. Meyer

Brown University
Division of Engineering
Providence 12, Rhode Island
Attention: Dr. Ronald F. Probst

University of California at Berkeley
Aeronautical Sciences Department
Room 203, Mechanics Building
Berkeley 4, California
Attention: Professor S. A. Schaaf

University of California
405 Hilgard Avenue
Los Angeles 24, California
Attention: Engineering and Mathematical
Sciences Library

University of California
Department of Engineering
Los Angeles 24, California
Attention: Professor A. F. Charwat
Attention: Professor John W. Miles
Attention: Dr. N. Rott

Case Institute of Technology
Department of Mechanical Engineering
University Circle
Cleveland 6, Ohio
Attention: Dr. G. Kuerti

Columbia University
Department of Mechanical Engineering
New York 27, N. Y.
Attention: Professor Robert A. Gross

Cornell University
Graduate School of Aeronautical Eng.
Ithaca, New York
Attention: Library
Attention: Dr. William R. Sears

University of Florida
Department of Aeronautical Eng.
Gainesville, Florida
Attention: Professor David T. Williams

Harvard University
Division of Eng. and App. Physics
Cambridge 38, Massachusetts
Attention: Dr. Howard W. Emmons

University of Illinois
Department of Aeronautical Engineering
Urbana, Illinois
Attention: Professor Harold O. Barthel
Attention: Dr. Allen I. Ormsbee

The Johns Hopkins University
Applied Physics Laboratory
8621 Georgia Avenue
Silver Spring, Maryland
Attention: Dr. L. L. Cronvich
Attention: Dr. F. K. Hill

The Johns Hopkins University
Department of Mechanics
Baltimore 18, Maryland
Attention: Dr. Francis H. Clauser
Attention: Dr. Stanley Corrsin
Attention: Professor L. S. G. Kovasznay

Lehigh University
Department of Physics
Bethlehem, Pennsylvania
Attention: Dr. Raymond J. Emrich

University of Maryland
Department of Aeronautical Engineering
College Park, Maryland
Attention: Professor S. F. Shen

University of Maryland
Institute for Fluid Dynamics and
Applied Mathematics
College Park, Maryland
Attention: Director
Attention: Professor J. M. Burgers
Attention: Professor Francis R. Hama
Attention: Professor S. I. Pai

Massachusetts Institute of Technology
Department of Aeronautics and Astronautics
Aerophysics Laboratory
560 Memorial Drive
Cambridge 39, Massachusetts
Attention: Dr. Morton Finston

Massachusetts Institute of Technology
Department of Mathematics
Cambridge 39, Massachusetts
Attention: Professor C. C. Lin
Attention: Dr. George B. Whitham

Massachusetts Institute of Technology
Department of Mechanical Engineering
Cambridge 39, Massachusetts
Attention: Dr. A. H. Shapiro
Attention: Dr. H. Guyford Stever
Room 3-174

Massachusetts Institute of Technology
Department of Aeronautics and Astronautics
Cambridge 39, Massachusetts
Attention: Professor E. Mollo-Christensen
Room 33-412
Attention: Dr. Leon Trilling
Room 33-412

University of Michigan
Ann Arbor, Michigan
Attention: Engineering Library

University of Michigan
Willow Run Laboratories
P. O. Box 618
Ann Arbor, Michigan
Attention: BAMIRAC Library
Mr. Richard Jamron, Head
Information Handling Group

University of Michigan
Aeronautical Engineering Laboratories
Aerodynamics Laboratory
North Campus
Ann Arbor, Michigan
Attention: Mr. James L. Amick

University of Michigan
Aeronautical Engineering Laboratories
Aircraft Propulsion Laboratory
North Campus
Ann Arbor, Michigan
Attention: Professor J. A. Nicholls

University of Michigan
Department of Aeronautical and
Astronautical Engineering
Ann Arbor, Michigan
Attention: Dr. Arnold M. Kuethe
Attention: Professor V. C. Liu
Attention: Professor William W. Willmarth

University of Michigan
Department of Physics
Ann Arbor, Michigan
Attention: Dr. O. Laporte

University of Minnesota
Institute of Technology
Rosemount Aeronautical Laboratories
Rosemount, Minnesota
Attention: Mrs. Linda Caldon,
Librarian

New York University
Institute of Mathematics and Mechanics
53 Washington Square, South
New York 12, N. Y.
Attention: Library

North Carolina State College
Department of Mechanical Engineering
Raleigh, North Carolina
Attention: Professor R. M. Pinkerton

Northwestern University
The Technological Institute
Evanston, Illinois
Attention: Professor Ali Buent Cambel

The Ohio State University
Department of Aeronautical and
Astronautical Engineering
2036 Neil Avenue
Columbus 10, Ohio
Attention: Professor John D. Lee
Attention: Professor Gavin L. VonEschen

Polytechnic Institute of Brooklyn
Aerodynamics Laboratory
527 Atlantic Avenue
Freeport, New York
Attention: Library
Attention: Professor Martin H. Bloom
Attention: Professor Antonio Ferri
Attention: Professor Paul A. Libby

Princeton University
School of Engineering
James Forrestal Research Center
Princeton, New Jersey
Attention: Library
Attention: Gas Dynamics Laboratory
Attention: Dr. Seymour Bogdonoff
Attention: Professor Sin-I Cheng
Attention: Dr. Luigi Crocco

Purdue University
School of Aeronautical and
Engineering Sciences
West Lafayette, Indiana
Attention: Aero. and Engineering
Sciences Library

Rensselaer Polytechnic Institute
Department of Aeronautical Engineering
Troy, New York
Attention: Library
Attention: Dr. Ting-Yi Li

University of Rochester
College of Engineering
Department of Mechanical Engineering
River Campus Station
Rochester 20, New York
Attention: Professor Martin Lessen

University of Southern California
Engineering Center
University Park
Los Angeles 7, California
Attention: Director
Attention: Dr. H. T. Yang

University of Southern California
Engineering Center
Aeronautical Laboratories Department
P. O. Box 1001
Oxnard, California
Attention: Mr. J. H. Carrington,
USCEC-ATL

Stanford University
Department of Aeronautical Engineering
Stanford, California
Attention: Professor Daniel Bershader
Attention: Dr. Milton Van Dyke
Attention: Professor Walter G. Vincenti

University of Texas
Defense Research Laboratory
P. O. Box 8029
Austin 12, Texas
Attention: Dr. M. J. Thompson

University of Virginia
Department of Physics
Charlottesville, Virginia
Attention: Dr. Jesse W. Beams

University of Washington
Department of Aeronautical Engineering
Seattle 5, Washington
Attention: Engineering Librarian
Attention: Professor R. E. Street

University of Wisconsin
Theoretical Chemistry Laboratory
P. O. Box 2127
Madison 5, Wisconsin
Attention: Dr. Joseph O. Hirschfelder

Yale University
Department of Mechanical Engineering
New Haven, Connecticut
Attention: Dr. Peter Wegener
Attention: Dr. Alan Kistler

Institute of the Aerospace Sciences
2 East 64th Street
New York 21, New York
Attention: Library

Industrial and Research Companies

Aeronautical Research Associates
of Princeton, Inc.
50 Washington Road
Princeton, New Jersey
Attention: Dr. Coleman duP. Donaldson

Aeronutronic
A Division of Ford Motor Company
Ford Road
P. O. Box 697
Newport Beach, California
Attention: Dr. L. L. Kavanau
Advanced Programs Staff

Aerospace Corporation, Inc.
P. O. Box 95085
Los Angeles 45, California
Attention: Dr. Chieh-Chien Chang
Attention: Dr. J. Logan, Director
2 copies
Attention: Dr. H. Mirels

ARO, Inc.
Arnold Air Force Station
Tennessee
Attention: AEDC Library
Attention: Dr. B. H. Goethert
Director of Engineering
Attention: TS(T1)

ARO, Inc.
von Karman Gas Dynamics Facility
Arnold Air Force Station
Tennessee
Attention: Dr. J. Lukasiewicz, Chief
Attention: Mr. J. Leith Potter,
Manager, Research Branch

AVCO-Everett Research Laboratory
2385 Revere Beach Parkway
Everett 49, Massachusetts
Attention: Barbara A. Spence,
Technical Librarian

AVCO Research and Advanced
Development Division
201 Lowell Street
Wilmington, Massachusetts
Attention: Mr. A. Kahane
Assistant Technical Director
Attention: Dr. Frederick R. Riddell,
Tech. Ass't. to Pres. -S. Tec.

Boeing Airplane Company
Aero-Space Division
Seattle 24, Washington
Attention: Library 13-84

CONVAIR
A Division of General Dynamics Corp.
Astronautics Division
P. O. Box 1128
San Diego 12, California
Attention: Mr. K. J. Bossart, Tech. Dir
Attention: Mr. W. B. Mitchell, 595-10

CONVAIR
A Division of General Dynamics Corp.
Scientific Research Laboratory
5001 Kearny Villa Road
San Diego 11, California
Attention: Mr. William H. Dorrance
Senior Staff Scientist
Mail Zone 1-162
Attention: Mr. Merwin Sibulkin
Staff Scientist

CONVAIR
A Division of General Dynamics Corp.
San Diego 12, California
Attention: Dr. H. Yoshihara
Chief of Fluid Dynamics Res.
Mail Zone 6-105

CONVAIR
A Division of General Dynamics Corp.
Aerospace Technology Section
P. O. Box 748
Fort Worth, Texas
Attention: Mr. R. C. Frost
Dept. 6-1
Mail Zone E63

CONVAIR
A Division of General Dynamics Corp.
Fort Worth, Texas
Attention: Mr. A. P. Madsen
Aerodynamics Group Eng.
Mail Zone E63
Attention: Mr. W. G. McMullen
Attention: Mr. Robert H. Widmer

CONVAIR
A Division of General Dynamics Corp.
Daingerfield, Texas
Attention: Mr. J. E. McMichael
Chief, Jet Engine Department

Cornell Aeronautical Laboratory, Inc.
P. O. Box 235
Buffalo 21, New York
Attention: Library
Attention: Dr. A. H. Flax
Attention: Mr. A. Hertzberg
Head, Aerodynamic Research

Douglas Aircraft Company, Inc.
Missiles and Space Systems
3000 Ocean Park Blvd.
Santa Monica, California
Attention: Library
Chief,
Aero/Astroynamics Section
2 copies
Attention: Mr. R. J. Gunkel
Chief,
Aero/Astroynamics Section

Douglas Aircraft Company, Inc.
827 Lapham Street
El Segundo, California
Attention: Dr. A. M. O. Smith

General Electric Company (MSVD)
Space Technology Center
Space Sciences Laboratory
King of Prussia, Pennsylvania
Attention: Dr. H. Lew

General Electric Company
Research Laboratory
P. O. Box 1088
Schenectady, New York
Attention: Dr. Henry T. Nagamatsu

Giannini Controls Corporation
1600 South Mountain Avenue
Duarte, California
Attention: Library

Grumman Aircraft Engineering Corp.
Bethpage, New York
Attention: Mr. Charles Tilgner, Jr.

Hughes Aircraft Company
Culver City, California
Attention: Mr. E. O. Marriott
Manager, Aerodynamics Dept.

Lockheed Aircraft Corporation
Lockheed Missiles and Space Company
Technical Information Center (50-14)
3251 Hanover Street
Palo Alto, California
Attention: Dr. W. A. Kozumplik
3 copies

Lockheed Aircraft Corporation
Lockheed Missiles and Space Company
P. O. Box 504
Sunnyvale, California
Attention: Mr. R. Smelt,
Chief Scientist

Lockheed Aircraft Corporation
Lockheed Missile and Space Company
Palo Alto, California
Attention: Mr. Maurice Tucker
Spacecraft and Missiles Research

Lockheed Aircraft Corporation
Missiles and Space Division
7701 Woodley Avenue
Van Nuys, California
Attention: Library

Lockheed Aircraft Corporation
Marietta, Georgia
Attention: Dr. W. F. Jacobs
Aerodynamics Dept. -72-07

Marquardt Aircraft Company
P. O. Box 2013 - South Annex
Van Nuys, California
Attention: Technical Library

The Martin Company
Baltimore 3, Maryland
Attention: Mr. K. Jarmolow
Mail No. J-3033
Attention: Dr. Mark V. Morkovin
Mail No. J-3033

McDonnell Aircraft Corporation
Lambert-Saint Louis Municipal Airport
P. O. Box 516
St. Louis 66, Missouri
Attention: Mr. Kendall Perkins

The RAND Corporation
1700 Main Street
Santa Monica, California
Attention: Librarian
Attention: Dr. Carl Gazley, Jr.
Attention: Mr. E. P. Williams
Aero-Astronautics Dept.

Republic Aviation Corporation
Farmingdale, Long Island, New York
Attention: Engineering Library
Attention: Mr. R. W. Perry
Chief, Re-Entry Simulation Lab.
Applied Research and Dev.

Space Technology Laboratories, Inc.
P. O. Box 95001
Los Angeles 45, California
Attention: Technical Information Center
Document Procurement
Bldg. C, Room 2412
Attention: Dr. James E. Broadwell
Aerodynamics Research Section
Attention: Dr. C. B. Cohen
Attention: Dr. Luois G. Dunn, President
Attention: Dr. Andrew G. Hammitt, Head
Aerodynamics Research Section
Attention: Mr. Ernest I. Pritchard
Attention: Dr. George E. Solomon

Sperry Utah Engineering Laboratory
Division of Sperry Rand Corporation
322 North 21st Street West
Salt Lake City 16, Utah
Attention: Mr. Malcolm L. Matthews

Systems Corporation of America
1007 Broxton Avenue
Los Angeles 24, California
Attention: Dr. Paul D. Arthur

United Aircraft Corporation
Research Laboratories
East Hartford 8, Connecticut
Attention: Mr. John G. Lee

Internal

Mr. Paul E. Baloga
Dr. Julian D. Cole
Dr. Donald E. Coles
Dr. Anthony Demetriades
Dr. Toshi Kubota
Professor Lester Lees
Dr. H. W. Liepmann
Dr. Clark B. Millikan
Dr. Barry L. Reeves
Dr. Anatol Roshko

Dr. Frank Marble
Dr. S. S. Penner
Dr. W. D. Rannie
Dr. Edward Zukoski

Dr. Harry Ashkenas
Mr. George Goranson
Dr. James M. Kendall
Dr. John Laufer
Dr. Thomas Vrebalovich
Mr. Richard Wood

Aeronautics Library (2)
Hypersonic Files (3)
Hypersonic Staff and Research Workers (20)